obvious features of DSH. Of note, DSH has only very rarely been reported outside of Japan and China. Moreover, even within known families segregating the DSH phenotype, a marked variability in expression is well recognized[31]. Although our findings do not necessarily implicate dysregulation of type I IFN in the DSH phenotype, they suggest that missense and null heterozygous mutations in *ADAR1* are consistent with both DSH (depending on, for example, ancestry) and with carrier or, in the case of the p.Gly1007Arg alteration, affected status for AGS. Thus, we believe that the lack of DSH skin features in our AGS cases and their heterozygous parents most likely relates to non-penetrance and/or variable expressivity due to ancestry or other genetic or non-genetic factors, and we predict that two individuals with DSH would have a 1 in 4 risk of having a child with AGS.

Because inosine is recognized as guanosine by the translation and splicing machineries, editing of adenosine to inosine can alter the protein-coding information of messenger RNA and the structural stability of dsRNA. The first identified ADAR-edited substrates were in codons, and ADARs were presumed to function primarily in proteome diversification. However, although codon editing is clearly important, it represents only a small fraction of editing events in the transcriptome, with editing sites in RNA derived from non-coding regions, most particularly Alu elements, being vastly more prevalent[32–35]. The biological function of such repetitive element editing is uncertain[36]. Recent studies have highlighted an antagonistic interaction between ADARs and the RNA interference machinery, suggesting that a pool of common RNA substrates is capable of engaging both pathways[37] and specifically implicating the binding properties of the p150 isoform of ADAR1, beyond its editing activity[28,38], in this relationship. How, then, does loss of ADAR1 activity lead to upregulation of type I IFN signaling? Theoretically, wild-type ADAR1 might edit specific currently undefined transcripts that are important in IFN regulation. Alternatively, and perhaps more likely, lack of editing in ADAR1-deficient cells may lead to an increase in immunoreactive dsRNA[37] and/or result in failure to generate inosine:uracil (IU)-dsRNA with an intrinsic function in suppressing IFN induction[39]. Considering insights derived from the study of TREX1, SAMHD1 and RNase H2, we speculate that ADAR1 has a role in the metabolism of retroelements and that a major contribution of ADARs to evolutionary fitness may be to regulate the accumulation of dsRNA generated from basally transcribed repetitive sequences within the genome.

URLs. UCSC Human Genome Browser, http://genome.ucsc.edu/; Ensembl, http://www.ensembl.org/; dbSNP, http://www.ncbi.nlm.nih.gov/projects/SNP/; Exome Variant Server, National Heart, Lung, and Blood Institute (NHLBI) Exome Sequencing Project (ESP) (accessed 21 March 2012), http://snp.gs.washington.edu/EVS/; PolyPhen, http://genetics.bwh.harvard.edu/pph/; SIFT, http://sift.jcvi.org/www/SIFT_enst_submit.html; Align GVGD, http://agvgd.iarc.fr/index.php; Clustal Omega, http://www.ebi.ac.uk/Tools/msa/clustalo/; Protein Data Bank (PDB), http://www.pdb.org/; Alamut, http://www.interactive-biosoftware.com/.

METHODS

Methods and any associated references are available in the online version of the paper.

Note: Supplementary information is available in the online version of the paper.

ACKNOWLEDGMENTS

We sincerely thank the participating families for the use of genetic samples and clinical information. We thank B. Hamel, H. Brunner and other clinical collaborators for contributing samples not included in the current manuscript, A.P. Jackson for highlighting the presence of intracranial calcification in individuals with DSH with a p.Gly1007Arg alteration in ADAR1 and D.B. Stetson and D.T. Bonthron for critical reading of the manuscript. D.B. Stetson (University of Washington) provided the *ADAR1* constructs used in the editing assays. We thank the NHLBI GO Exome Sequencing Project and its ongoing studies that produced and provided exome variant calls for comparison: the Lung GO Sequencing Project (HL-102923), the Women's Health Initiative (WHI) Sequencing Project (HL-102924), the Broad GO Sequencing Project (HL-102925), the Seattle GO Sequencing Project (HL-102926) and the Heart GO Sequencing Project (HL-103010). Y.J.C. acknowledges the Manchester National Institute for Health Research (NIHR) Biomedical Research Centre. The research leading to these results has received funding from the European Union's Seventh Framework Programme (FP7/2007-2013) under grant agreement 241779 and from the Great Ormond Street Hospital Children's Charity.

AUTHOR CONTRIBUTIONS

G.I.R. performed quantitative PCR analysis. P.R.K. performed protein blot analysis. G.M.A.F. performed cell culture and interferon stimulation experiments with assistance from G.I.R. and T.A.B. M.S. performed Sanger sequencing with assistance from M.Z., G.M.A.F. and E.M.J. G.I.R. analyzed sequence data. M.S. and G.M.A.F. undertook microsatellite genotyping. J.E.D. and S.S.B. undertook analysis of the exome sequence data. J.H.L. was responsible for neuroradiological phenotyping. P.L. and F.R. measured interferon activity in affected individuals. M.A.O., L.P.K., S.M.G. and N.M.M. carried out ADAR1 editing assays. T.S. and M.K. provided the DSH RNA samples. S.C.L. and P.J.M. carried out ADAR1 structural analysis. Y.J.C. designed and supervised the project and wrote the manuscript with support from G.I.R. C.A.B., R.B., E.B., P.A.B., L.A.B., M.C., C.D.L., P.d.L., M.d.T., I.D., E.F., A.G.-C., A.H., R.K., J.-P.S.-M.L., C.M.L., A.M.M., W.M., C.M., I.O., S.O., P.P., M.R., R.A.R., J.L.S., K.S., T.Y.T., W.G.v.d.M., A.V., G.V., E.L.W., E. Wassmer and E. Whittaker identified subjects with AGS or assisted with related clinical and laboratory studies.

COMPETING FINANCIAL INTERESTS

The authors declare no competing financial interests.

Published online at http://www.nature.com/doifinder/10.1038/ng.2414.
Reprints and permissions information is available online at http://www.nature.com/reprints/index.html.

1. Crow, Y.J. & Livingston, J.H. Aicardi-Goutières syndrome: an important Mendelian mimic of congenital infection. *Dev. Med. Child Neurol.* **50**, 410–416 (2008).
2. Lebon, P. *et al.* Intrathecal synthesis of interferon-α in infants with progressive familial encephalopathy. *J. Neurol. Sci.* **84**, 201–208 (1988).
3. Crow, Y.J. *et al.* Mutations in the gene encoding the 3′-5′ DNA exonuclease TREX1 cause Aicardi-Goutières syndrome at the *AGS1* locus. *Nat. Genet.* **38**, 917–920 (2006).
4. Crow, Y.J. *et al.* Mutations in genes encoding ribonuclease H2 subunits cause Aicardi-Goutières syndrome and mimic congenital viral brain infection. *Nat. Genet.* **38**, 910–916 (2006).
5. Rice, G.I. *et al.* Mutations involved in Aicardi-Goutières syndrome implicate SAMHD1 as regulator of the innate immune response. *Nat. Genet.* **41**, 829–832 (2009).
6. Goldstone, D.C. *et al.* HIV-1 restriction factor SAMHD1 is a deoxynucleoside triphosphate triphosphohydrolase. *Nature* **480**, 379–382 (2011).
7. Rice, G. *et al.* Clinical and molecular phenotype of Aicardi-Goutières syndrome. *Am. J. Hum. Genet.* **81**, 713–725 (2007).
8. Rice, G. *et al.* Heterozygous mutations in *TREX1* cause familial chilblain lupus and dominant Aicardi-Goutières syndrome. *Am. J. Hum. Genet.* **80**, 811–815 (2007).
9. Ramantani, G. *et al.* Expanding the phenotypic spectrum of lupus erythematosus in Aicardi-Goutières syndrome. *Arthritis Rheum.* **62**, 1469–1477 (2010).
10. Haaxma, C.A. *et al.* A *de novo* p.Asp18Asn mutation in *TREX1* in a patient with Aicardi-Goutières syndrome. *Am. J. Med. Genet. A.* **152A**, 2612–2617 (2010).
11. Stetson, D.B., Ko, J.S., Heidmann, T. & Medzhitov, R. Trex1 prevents cell-intrinsic initiation of autoimmunity. *Cell* **134**, 587–598 (2008).
12. Gall, A. *et al.* Autoimmunity initiates in nonhematopoietic cells and progresses via lymphocytes in an interferon-dependent autoimmune disease. *Immunity* **36**, 120–131 (2012).
13. Yan, N. *et al.* The cytosolic exonuclease TREX1 inhibits the innate immune response to human immunodeficiency virus type 1. *Nat. Immunol.* **11**, 1005–1013 (2010).
14. Laguette, N. *et al.* SAMHD1 is the dendritic- and myeloid-cell-specific HIV-1 restriction factor counteracted by Vpx. *Nature* **474**, 654–657 (2011).
15. Hrecka, K. *et al.* Vpx relieves inhibition of HIV-1 infection of macrophages mediated by the SAMHD1 protein. *Nature* **474**, 658–661 (2011).
16. Lahouassa, H. *et al.* SAMHD1 restricts the replication of human immunodeficiency virus type 1 by depleting the intracellular pool of deoxynucleoside triphosphates. *Nat. Immunol.* **13**, 223–228 (2012).

17. Genovesio, A. *et al.* Automated genome-wide visual profiling of cellular proteins involved in HIV infection. *J. Biomol. Screen.* **16**, 945–958 (2011).
18. Beck-Engeser, G.B., Eilat, D. & Wabl, M. An autoimmune disease prevented by anti-retroviral drugs. *Retrovirology* **8**, 91 (2011).
19. Hartner, J.C., Walkley, C.R., Lu, J. & Orkin, S.H. ADAR1 is essential for the maintenance of hematopoiesis and suppression of interferon signaling. *Nat. Immunol.* **10**, 109–115 (2009).
20. Crow, Y.J. Type I interferonopathies: a novel set of inborn errors of immunity. *Ann. NY Acad. Sci.* **1238**, 91–98 (2011).
21. Hogg, M., Paro, S., Keegan, L.P. & O'Connell, M.A. RNA editing by mammalian ADARs. *Adv. Genet.* **73**, 87–120 (2011).
22. George, C.X. & Samuel, C.E. Human RNA-specific adenosine deaminase *ADAR1* transcripts possess alternative exon 1 structures that initiate from different promoters, one constitutively active and the other interferon inducible. *Proc. Natl. Acad. Sci. USA* **96**, 4621–4626 (1999).
23. Herbert, A. *et al.* A Z-DNA binding domain present in the human editing enzyme, double-stranded RNA adenosine deaminase. *Proc. Natl. Acad. Sci. USA* **94**, 8421–8426 (1997).
24. Miyamura, Y. *et al.* Mutations of the RNA-specific adenosine deaminase gene (*DSRAD*) are involved in dyschromatosis symmetrica hereditaria. *Am. J. Hum. Genet.* **73**, 693–699 (2003).
25. Li, M. *et al.* Mutational spectrum of the *ADAR1* gene in dyschromatosis symmetrica hereditaria. *Arch. Dermatol. Res.* **302**, 469–476 (2010).
26. Tojo, K. *et al.* Dystonia, mental deterioration, and dyschromatosis symmetrica hereditaria in a family with *ADAR1* mutation. *Mov. Disord.* **21**, 1510–1513 (2006).
27. Kondo, T. *et al.* Dyschromatosis symmetrica hereditaria associated with neurological disorders. *J. Dermatol.* **35**, 662–666 (2008).
28. Heale, B.S. *et al.* Editing independent effects of ADARs on the miRNA/siRNA pathways. *EMBO J.* **28**, 3145–3156 (2009).
29. Cho, D.S. *et al.* Requirement of dimerization for RNA editing activity of adenosine deaminases acting on RNA. *J. Biol. Chem.* **278**, 17093–17102 (2003).
30. Abdel-Salam, G.M. *et al.* Chilblains as a diagnostic sign of Aicardi-Goutières syndrome. *Neuropediatrics* **41**, 18–23 (2010).
31. Kondo, T. *et al.* Six novel mutations of the *ADAR1* gene in patients with dyschromatosis symmetrica hereditaria: histological observation and comparison of genotypes and clinical phenotypes. *J. Dermatol.* **35**, 395–406 (2008).
32. Levanon, E.Y. *et al.* Systematic identification of abundant A-to-I editing sites in the human transcriptome. *Nat. Biotechnol.* **22**, 1001–1005 (2004).
33. Athanasiadis, A., Rich, A. & Maas, S. Widespread A-to-I RNA editing of Alu-containing mRNAs in the human transcriptome. *PLoS Biol.* **2**, e391 (2004).
34. Blow, M., Futreal, P.A., Wooster, R. & Stratton, M.R. A survey of RNA editing in human brain. *Genome Res.* **14**, 2379–2387 (2004).
35. Kim, D.D. *et al.* Widespread RNA editing of embedded Alu elements in the human transcriptome. *Genome Res.* **14**, 1719–1725 (2004).
36. Hundley, H.A. & Bass, B.L. ADAR editing in double-stranded UTRs and other noncoding RNA sequences. *Trends Biochem. Sci.* **35**, 377–383 (2010).
37. Wu, D., Lamm, A.T. & Fire, A.Z. Competition between ADAR and RNAi pathways for an extensive class of RNA targets. *Nat. Struct. Mol. Biol.* **18**, 1094–1101 (2011).
38. Yang, W. *et al.* ADAR1 RNA deaminase limits short interfering RNA efficacy in mammalian cells. *J. Biol. Chem.* **280**, 3946–3953 (2005).
39. Vitali, P. & Scadden, A.D. Double-stranded RNAs containing multiple IU pairs are sufficient to suppress interferon induction and apoptosis. *Nat. Struct. Mol. Biol.* **17**, 1043–1050 (2010).
40. Gallo, A., Keegan, L.P., Ring, G.M. & O'Connell, M.A. An ADAR that edits transcripts encoding ion channel subunits functions as a dimer. *EMBO J.* **22**, 3421–3430 (2003).

[1]Manchester Academic Health Science Centre, University of Manchester, Genetic Medicine, Manchester, UK. [2]Medical Research Council (MRC) Human Genetics Unit, Institute of Genetics and Molecular Medicine (IGMM), University of Edinburgh, Edinburgh, UK. [3]Department of Molecular and Human Genetics, Baylor College of Medicine, Houston, Texas, USA. [4]Department of Developmental Neuroscience, Istituto di Ricovero e Cura a Carattere Scientifico (IRCCS) Stella Maris, Pisa, Italy. [5]Laboratory of Molecular Medicine, Department of Neuroscience, Bambino Gesù Children's Research Hospital, Rome, Italy. [6]University College London (UCL) Institute of Child Health, London, UK. [7]Birmingham Women's National Health Service (NHS) Foundation Trust, Birmingham, UK. [8]Department of Child Neurology and Psychiatry, A Manzoni Hospital, Lecco, Italy. [9]Nutrition and Metabolism Unit, Hôpital Universitaire des Enfants Reine Fabiola (ULB), Brussels, Belgium. [10]Reference Center of Metabolic Diseases, Hôpital Necker–Enfants Malades, Paris Descartes University, Paris, France. [11]Pediatric Neurology Unit, Hospital Vall d'Hebron, Barcelona, Spain. [12]Neuropediatric Unit, Assistance Publique–Hôpitaux de Paris (AP-HP), Paris V Descartes University, Necker Hospital, Paris, France. [13]Mother and Child Department, Unit of Child Neurology and Psychiatry, Civil Hospital, University of Brescia, Brescia, Italy. [14]Department of Neurology, Hospital Sant Joan de Déu (HSJD), Barcelona, Spain. [15]El Centro de Investigación Biomédica en Red de Enfermedades Raras (CIBER-ER), Instituto de Salud Carlos III, Madrid, Spain. [16]Department of Medical Genetics, Oslo University Hospital, National Hospital, Oslo, Norway. [17]Department of Dermatology, Yamagata University Faculty of Medicine, Yamagata, Japan. [18]Department of Neurology, Alder Hey Children's NHS Foundation Trust, Liverpool, UK. [19]General Neurology & Complex Motor Disorders Service, Evelina Children's Hospital, Guy's & St. Thomas' NHS Foundation Trust, London, UK. [20]Department of Neurosciences and Behavior Sciences, School of Medicine of Ribeirão Preto, University of São Paulo, São Paulo, Brazil. [21]North East Thames Regional Genetics Service, Great Ormond Street Hospital for Children, London, UK. [22]Département de Génétique et Cytogénétique, AP-HP, Groupe Hospitalier Pitié–Salpêtrière, Paris, France. [23]Service de Neuropédiatrie, AP-HP, Hopital Armand Trousseau, Paris, France. [24]Centre de Déficience des Déficiences Intellectuelles de Causes Rares, Paris, France. [25]Child Neurology and Psychiatry Unit, IRCCS C Mondino National Institute of Neurology Foundation, Pavia, Italy. [26]Department of Neurology, Great Ormond Street Hospital, London, UK. [27]Section of Child Neurology, Women and Children's Division, Oslo University Hospital, Oslo, Norway. [28]Service de Virologie, Paris Descartes University, AP-HP, Hopital Cochin St. Vincent de Paul, Paris, France. [29]Department of Neurology, Children's National Medical Center, Washington, DC, USA. [30]Institute of Medical Genetics, University of Zurich, Schwerzenbach, Switzerland. [31]Victorian Clinical Genetics Services, Murdoch Children's Research Institute, Royal Children's Hospital, Melbourne, Victoria, Australia. [32]Paediatric Department, Nobles Hospital, Strang, UK. [33]Neurology Department, Royal Manchester Children's Hospital, Manchester, UK. [34]North West Thames Regional Genetics Service, North West London Hospitals NHS Trust, Harrow, UK. [35]Neurology Department, Birmingham Children's Hospital, Birmingham, UK. [36]Academic Department of Paediatrics, Imperial College London, London, UK. [37]Department of Paediatric Neurology, Leeds General Infirmary, Leeds, UK. [38]Institute of Structural and Molecular Biology, School of Biological Sciences, The University of Edinburgh, Edinburgh, UK. [39]Faculty of Life Sciences, University of Manchester, Manchester, UK. Correspondence should be addressed to Y.J.C. (yanickcrow@mac.com).

ONLINE METHODS

Affected individuals and families. All affected individuals included in this study had a clinical diagnosis of AGS that was based on the presence of early-onset encephalopathy (at <18 months of age), negative investigations for common prenatal infections, intracranial calcification with or without white matter changes in a typical distribution, elevated levels of IFN-α with or without pterins in the cerebrospinal fluid and/or chilblains. Clinical information and samples were obtained with informed consent. The study was approved by the Leeds (East) Research Ethics Committee (reference 10/H1307/132).

Exome sequencing. Genomic DNA was extracted from lymphocytes from affected individuals and parents by standard techniques. For whole-exome analysis, targeted enrichment and sequencing were performed on 3 μg of DNA extracted from the peripheral blood of four individuals (AGS81_P1, AGS125, AGS163 and AGS219). Enrichment was undertaken using the 38 Mb SureSelect Human All Exon kit (Agilent) following the manufacturer's protocol, and samples were paired-end sequenced on an Illumina HiSeq 2000. Sequence data were mapped using BWA (Burrows-Wheeler Aligner) against the hg18 (NCBI Build 36) human genome as a reference. Variants were called using SOAPsnp and SOAPindel (from the Short Oligonucleotide Analysis Package) with medium stringency and were then filtered for those with greater than 5× coverage.

Sanger sequencing. Primers were designed to amplify the coding exons of *ADAR1* (**Supplementary Table 8**). Purified PCR amplification products were sequenced using BigDye terminator chemistry and an ABI 3130 DNA sequencer. Mutations were annotated on the basis of the reference cDNA sequence NM_001111.4, with nucleotide numbering beginning from the first A in the initiating ATG codon.

Gene expression analysis. The expression of 15 genes known to be interferon stimulated was assessed in whole blood. Total RNA was extracted from whole blood using the PAXgene RNA isolation kit (PreAnalytix). RNA concentration was assessed using a spectrophotometer (FLUOstar Omega, Labtech). Quantitative RT-PCR analysis was performed using TaqMan Universal PCR Master Mix (Applied Biosystems) and cDNA derived from 40 ng of total RNA. The relative abundance of target transcripts, measured using TaqMan probes for *Ly6E* (Hs00158942_m1), *MX1* (Hs00895598_m1), *USP18* (Hs00276441_m1), *RSAD2* (Hs01057264_m1), *OAS1* (Hs00973637_m1), *IFI44L* (Hs00199115_m1), *IFI27* (Hs01086370_m1), *ISG15* (Hs00192713_m1), *IFIT1* (Hs00356631_g1), *IFI44* (Hs00197427_m1), *IFI6* (Hs00242571_m1), *SIGLEC1* (Hs00988063_m1), *IFIT3* (Hs00155468_m1), *IRF7* (Hs00185375_m1) and *STAT1* (Hs01013989_m1), was normalized to the expression level of *HPRT1* (Hs03929096_g1) and *18s* (Hs999999001_s1) and assessed with Applied Biosystems StepOne Software v2.1. Statistical significance between groups was determined by *t* tests using DataAssist v2.0 (Applied Biosystems). Data from affected individuals are expressed relative to the average of nine normal controls. A subset of the six most highly expressed ISGs (*RSAD2*, *IFI44L*, *IFI27*, *ISG15*, *IFIT1* and *SIGLEC1*) were measured in 20 controls, 10 *ADAR1* mutation–positive cases, 6 sets of *ADAR1* heterozygous parents and 18 individuals with *ADAR1* mutation–positive DSH. RNA from individuals with DSH was extracted using the QIAamp RNA Blood Mini kit (Qiagen), and cDNA was derived as above. Statistical significance between groups was determined by Kruskall Wallis tests using GraphPad Prism 5. The median fold change of the 6 ISGs compared to the median of the 20 healthy controls was used to create a score for each affected individual, similarly to previously described methods[41,42].

Interferon stimulation. EBV-transformed lymphoblastoid cells from affected individuals and controls were counted using a Bright-Line Hemacytometer (Sigma). We then transferred 10 ml of cells at a concentration of 1×10^6 cells/ml to each of two T25 flasks per cell line. One flask for each cell line was stimulated with 1,000 international units (IU)/ml of human IFN-α (human Intron A, Shering-Plough) for 24 h.

Protein analysis. Whole-cell lysates were prepared from lymphoblastoid cells (1×10^7 cells per sample) using 10 mM EDTA–RIPA buffer containing protease inhibitors (Roche). For protein blot analysis, 10 μg of total protein was loaded onto 8% SDS-PAGE gels, and electrophoresis was performed using the Mini-PROTEAN system (Bio-Rad Laboratories). Following wet-blotting transfer of the proteins onto PVDF membrane (Amersham), non-specific antibody binding was blocked using 5% normal goat serum (Vector Laboratories) and 2% BSA (Sigma) in 0.1% TBS-Tween (Sigma) overnight at 4 °C with gentle agitation. Rabbit primary antibody to ADAR (Sigma, Prestige Antibodies, HPA003890) was incubated with the membranes for 2 h at room temperature using a dilution of 1:800. As a loading control, membranes were incubated with a 1:4,000 dilution of rabbit primary antibody to α/β-tubulin (Cell Signaling Technology, 2148). Horseradish peroxidase (HRP)-labeled goat secondary antibody to rabbit (1:10,000; Cell Signaling Technology, 7074) was incubated with the membranes for 1 h at room temperature to detect both ADAR1 and tubulin antibodies. Signal was detected using a 1:10 dilution of Enhanced Chemiluminescence reagents (Lumigen).

Microsatellite genotyping. To exclude non-paternity, informative polymorphic microsatellite markers on chromosomes 3 (D3S3640 and D3S3560), 11 (D11S913 and D11S1889) and 20 (D20S847, D20S896 and D20S843) were genotyped using DNA from AGS150, AGS475, their parents and an unrelated control sample. DNA samples were amplified by standard PCR (primer sequences available upon request). Each amplicon was mixed with Hi-Di Formamide (Applied Biosystems) and 500 ROX Size Standard (Applied Biosystems) and run on the Genetic Analyzer 3010 capillary electrophoresis system. Results were analyzed with GeneMapper v4.1 software (Applied Biosystems).

Editing assays. Transient transfections were performed with slight adaptations to a previously described protocol[28] in 24-well plates seeded the day before transfection with 0.14×10^6 cells using Lipofectamine 2000 and OptiMEM I reduced serum medium. Cells were transfected with 500 ng of plasmid expressing a known ADAR1 editing substrate, miR376-a2, together with 500 ng of plasmid expressing wild-type ADAR1 p110 protein or the mutants Ala870Thr, Ile872Thr, Arg892His, Lys999Asn, Gly1007Arg and Asp1113His, for which coding sequences had been subcloned into the pcDNA3.1 expression vector. Reduced serum medium was replaced after 6 h with DMEM, and cells were harvested after 48 h. Total RNA was extracted with TRIzol reagent (Invitrogen), purified and treated with TURBO DNase (Ambion) and RNasin Plus RNase Inhibitor (Promega). Reverse transcription was carried out using SuperScript II and random hexamers, and cDNA was amplified by PCR with Platinum Taq DNA polymerase and specific primers for pri-miR376-a2 (**Supplementary Table 8**). The 300-bp PCR product was purified with exonuclease in combination with shrimp alkaline phosphatase (SAP) before sequencing. RNA editing of the pri-miR376-a2 transcript was identified as an adenosine-to-guanine change within the cDNA sequence, and the editing level was expressed as a percentage. Peak heights were measures for edited (G) and unedited (A), the editing ratio percentage was calculated by $(G / (A + G)) \times 100$. Results are the average of two separate experiments. Statistical significance between groups was determined by two-tailed *t* tests using Excel.

Protein modeling. The ADAR1 substitutions p.Ala870Thr, p.Ile872Thr, p.Arg892His, p.Lys999Asn, p.Gly1007Arg, p.Tyr1112Phe and p.Asp1113His all fall within the adenosine deaminase domain. No crystal structure is available for this domain in human ADAR1; thus, a comparative model was constructed using the deaminase domain of human ADAR2 (Protein Data Bank (PDB) 1zy7)[43]. The sequences of ADAR1 and ADAR2 were aligned using ClustalW[44], and 25 models were built using Modeller[45]. The model with the lowest discrete optimized protein energy (DOPE) score was selected (representing the most probable model judged by the fit to the Modeller statistical potential). Residues 975–996 could not be modeled accurately, as they have no equivalent in ADAR2; for this reason, these residues were not analyzed further. Models of mutations were built using KiNG[46], hydrogen atoms were added with Reduce[47], and all-atom contacts were calculated with Probe[48]. In each case, all low-energy rotamers[49] were considered, and the rotamer with the best Probe score was used. We assumed a similar binding mode for ADAR2 to that described for the tRNA deaminase–tRNA anticodon complex[50], allowing us to orientate the deaminase domain of ADAR2 on dsRNA and position it relative to the ADAR2-dsRBD2 complex[51]. The crystal structure of the ADAR1

Z-DNA–binding domain[52] (PDB 1qbj) was used to analyze the likely structural effect of the p.Pro193Ala substitution. As the side chain of alanine has no degrees of freedom from rotatable dihedral angles, the position of the side chain is determined by the conformation of the protein backbone.

41. Yao, Y. *et al.* Development of potential pharmacodynamic and diagnostic markers for anti-IFN-α monoclonal antibody trials in systemic lupus erythematosus. *Hum. Genomics Proteomics* **2009**, 374312 (2009).
42. Higgs, B.W. *et al.* Patients with systemic lupus erythematosus, myositis, rheumatoid arthritis and scleroderma share activation of a common type I interferon pathway. *Ann. Rheum. Dis.* **70**, 2029–2036 (2011).
43. Macbeth, M.R. *et al.* Inositol hexakisphosphate is bound in the ADAR2 core and required for RNA editing. *Science* **309**, 1534–1539 (2005).
44. Larkin, M.A. *et al.* Clustal W and Clustal X version 2.0. *Bioinformatics* **23**, 2947–2948 (2007).
45. Sali, A. & Blundell, T.L. Comparative protein modelling by satisfaction of spatial restraints. *J. Mol. Biol.* **234**, 779–815 (1993).
46. Chen, V.B., Davis, I.W. & Richardson, D.C. KING (Kinemage, Next Generation): a versatile interactive molecular and scientific visualization program. *Protein Sci.* **18**, 2403–2409 (2009).
47. Word, J.M., Lovell, S.C., Richardson, J.S. & Richardson, D.C. Asparagine and glutamine: using hydrogen atom contacts in the choice of side-chain amide orientation. *J. Mol. Biol.* **285**, 1735–1747 (1999).
48. Word, J.M. *et al.* Visualizing and quantifying molecular goodness-of-fit: small-probe contact dots with explicit hydrogen atoms. *J. Mol. Biol.* **285**, 1711–1733 (1999).
49. Lovell, S.C., Word, J.M., Richardson, J.S. & Richardson, D.C. The penultimate rotamer library. *Proteins* **40**, 389–408 (2000).
50. Losey, H.C., Ruthenburg, A.J. & Verdine, G.L. Crystal structure of *Staphylococcus aureus* tRNA adenosine deaminase TadA in complex with RNA. *Nat. Struct. Mol. Biol.* **13**, 153–159 (2006).
51. Stefl, R. *et al.* The solution structure of the ADAR2 dsRBM-RNA complex reveals a sequence-specific readout of the minor groove. *Cell* **143**, 225–237 (2010).
52. Schwartz, T. *et al.* Crystal structure of the Zα domain of the human editing enzyme ADAR1 bound to left-handed Z-DNA. *Science* **284**, 1841–1845 (1999).

Journal of Dermatological Science 70 (2013) 26–33

Contents lists available at SciVerse ScienceDirect

Journal of Dermatological Science

journal homepage: www.elsevier.com/jds

Immunolocalization and translocation of aquaporin-5 water channel in sweat glands

Risako Inoue [a,b], Eisei Sohara [b], Tatemitsu Rai [b], Takahiro Satoh [c], Hiroo Yokozeki [a], Sei Sasaki [b], Shinichi Uchida [b,*]

[a] Department of Dermatology, Graduate School of Medical and Dental Sciences, Tokyo Medical and Dental University, Tokyo, Japan
[b] Department of Nephrology, Graduate School of Medical and Dental Sciences, Tokyo Medical and Dental University, Tokyo, Japan
[c] Department of Dermatology, National Defense Medical College, Saitama, Japan

ARTICLE INFO

Article history:
Received 17 October 2012
Received in revised form 21 January 2013
Accepted 31 January 2013

Keywords:
Aquaporin
Sweat gland
Trafficking
Anoctamin

ABSTRACT

Background: Aquaporin-5 (AQP5) is a member of the water channel protein family. Although AQP5 was shown to be present in sweat glands, the presence or absence of regulated intracellular translocation of AQP5 in sweat glands remained to be determined.
Objective: We investigated whether AQP5 in sweat glands translocated during sweating, and also sought to determine the intracellular signal that triggers this translocation.
Methods: Immunofluorescent analyses of AQP5 in mouse and human sweat glands were performed. Madin-Darby Canine kidney (MDCK) cell lines stably expressing human AQP5 were generated, and the regulated translocation of AQP5 in the polarized cells was assessed by immunofluorescent analysis and biotinylation assays.
Results: AQP5 showed rapid translocation to the apical membranes during sweating. In human eccrine sweat glands, immunoreactive AQP5 was detected in the apical membranes and the intercellular canaliculi of secretory coils, and in the basolateral membranes of the clear cells. Treatment of human AQP5-expressing MDCK cells with calcium ionophore A23187 resulted in a twofold increase of AQP5 in the apical membranes within 5 min.
Conclusion: The regulated AQP5 translocation may contribute to sweat secretion by increasing the water permeability of apical plasma membranes of sweat glands.

1. Introduction

Secretion of fluid is the principal function of eccrine sweat glands. An eccrine sweat gland is a single tubular structure consisting of a secretory portion and a ductal portion. In the secretory portion, primary fluid, i.e., primary sweat, is secreted onto the lumen by active salt transport followed by movement of water, and the fluid transits through the duct where salt reabsorption occurs [1,2]. Dyshidrosis, including hyperhidrosis, hypohidrosis and anhidrosis, is a serious problem that can have a severe impact on daily life. For example, primary focal hyperhidrosis is a disorder of excessive sweating that occurs in the palms, soles, axillae and craniofacial region. This condition results in occupational, psychological and physical impairment and potential social stigmatization [3,4]. Patients have several treatment options [5], but these treatments have complications and limitations [6]. Patients with obstinate dyshidrosis or who experience serious side effects are desperate for new treatments. In order to develop new treatments, further understanding of the regulation of sweating, especially the regulation of fluid movement, is required.

Aquaporins (AQPs) are a family of integral membrane channel proteins that allow the rapid movement of water across the plasma membrane. Thirteen members of the AQP family (AQP0–AQP12) have been identified in mammals to date, and these proteins are expressed in various fluid-transporting epithelia with a distinct tissue-specific pattern [7]. Although there have been a few reports regarding the presence of AQP5 in sweat glands [8–13], its involvement in sweating is not well understood.

In the present study, we focused on translocation of AQP5 in sweat glands. By immunofluorescent studies of AQP5 in the sweat glands, we found that AQP5 showed apical translocation during sweating. We then generated Madin-Darby canine kidney (MDCK) cell lines stably expressing human AQP5 (hAQP5), and found that the intracellular calcium might mediate this translocation.

* Corresponding author at: 1-5-45 Yushima, Bunkyo-ku, Tokyo 113-8510, Japan. Tel.: +81 3 5803 5214; fax: +81 3 5803 5215.
E-mail address: suchida.kid@tmd.ac.jp (S. Uchida).

0923-1811/$36.00
http://dx.doi.org/10.1016/j.jdermsci.2013.01.013

2. Materials and methods

2.1. Antibodies and chemical reagents

Primary antibodies used were: rabbit monoclonal anti-AQP5 (ab93230, Abcam, Cambridge, MA, USA), goat polyclonal anti-AQP5 (sc-9890, Santa Cruz Biotechnology, CA, USA), mouse monoclonal anti-Na^+/K^+ATPase (sc-21712, Sigma–Aldrich, St. Louis, MO, USA), and rabbit anti-anoctamin-1 (ANO1) antibody generated in our laboratory using the antigen peptide (NH_2–C + GDGSPVPSYEYHGDAL–COOH, corresponding to amino acid residues 941–956 of mouse ANO1). Secondary antibodies used for immunofluorescence were Alexa Fluor 488- or 546-conjugated anti-IgG antibodies (Invitrogen, Carlsbad, CA, USA). Alkaline phosphatase-conjugated anti-rabbit IgG antibody (S373B, Promega, Madison, WI, USA) was used as the secondary antibody for immunoblotting.

2.2. Animal study

We used C57BL6/J mice at the age of 24 weeks. Sweating was detected using a modified Minor method; mouse paws were painted with 3% iodine in ethanol, coated with 80% starch solution in olive oil and observed. To make the mice sweat, we simply held the mice in our hands without anesthesia. To obtain non-sweating mice, we intraperitoneally anesthetized the mice with Inactin (Dainippon Sumitomo Pharma, Osaka, Japan). In the sweating group, we could see spots appearing on their paws soon after holding. When the number and the size of the spots were still increasing (5 min after we started holding), the mice were rapidly anesthetized with diethyl ether (Sigma–Aldrich), and the paws of the mice in both groups were quickly removed and frozen in liquid nitrogen. All procedures and experiments were designed according to the Declaration of Helsinki Principles and approved by the Animal Care and Use Committee of Tokyo Medical and Dental University.

2.3. Immunofluorescence studies in mouse and human sweat glands

Specimens of healthy skin were taken from patients after surgery under local anesthesia with informed consent in accordance with the declaration of Helsinki Principles. The ethical committee of Tokyo Medical and Dental University approved this study. The specimens were fixed overnight in 10% Formalin Neutral Buffer Solution (Wako, Osaka, Japan) and embedded in paraffin. After antigen retrieval and blocking with 1% BSA, the sections were incubated overnight with primary antibodies. Immunofluorescent images were obtained by using an LSM confocal microscope (Carl Zeiss Japan, Tokyo, Japan). For quantification of AQP5 labeling, we evaluated the intensity of AQP5 immunofluorescence in each cross section of the coils using LSM5 software version 4.0. The percentage of AQP5 signal in the apical membranes to total signal in each coil was calculated.

2.4. Generation of MDCK cell lines stably expressing non-tagged human AQP5

hAQP5 cDNA without any tag sequence was amplified by PCR using hAQP5 cDNA in pDNOR201 (FLJ81272AAAF, NITE Biological Resource Center, Chiba, Japan) as a template, and was then subcloned into the pcDNA3.1 (+) vector (Invitrogen). Stably transfected MDCK cell clones were isolated in a selection medium containing 1.2 mg/ml G418 (Sigma–Aldrich) and screened by Western blot analysis using the anti-human AQP5 antibody.

2.5. Immunoblotting

The cells were lysed in a lysis buffer (1% Triton X-100, 50 mM Tris–HCl, 5 mM EDTA, 150 mM NaCl) for 30 min at 37 °C, and mixed with 2× Laemmli sample buffer for 15 min at room temperature to denature the proteins. The samples were run on a 10–20% SDS–PAGE gel (Wako) and blotted onto nitrocellulose membranes (RPN2020D, Amersham, Buckinghamshire, UK). Signals were detected using the WesternBlue chromogenic substrate (Promega).

2.6. Side-specific biotinylation assay

MDCK cells stably expressing hAQP5 were seeded on polycarbonate filters (Corning, NY, USA) until they formed a confluent monolayer. After treatment with or without 10 μM calcium ionophore A23187, Sulfo-NHS-Biotin (0.5 mg/ml) (Thermo Scientific, Waltham, MA, USA) was applied to the apical or the basolateral surface for 20 min. The subsequent procedures are described in our previous paper [14]. When side-specific biotinylated AQP5 protein was analyzed, an immunoreaction-enhancing solution (NKB101, TOYOBO, Osaka, Japan) was used. Band intensity was analyzed using Image J (NIH, Bethesda, MD, USA).

2.7. Statistical methods

Statistical analyses were performed using the Student's *t*-test. $P < 0.05$ was considered statistically significant.

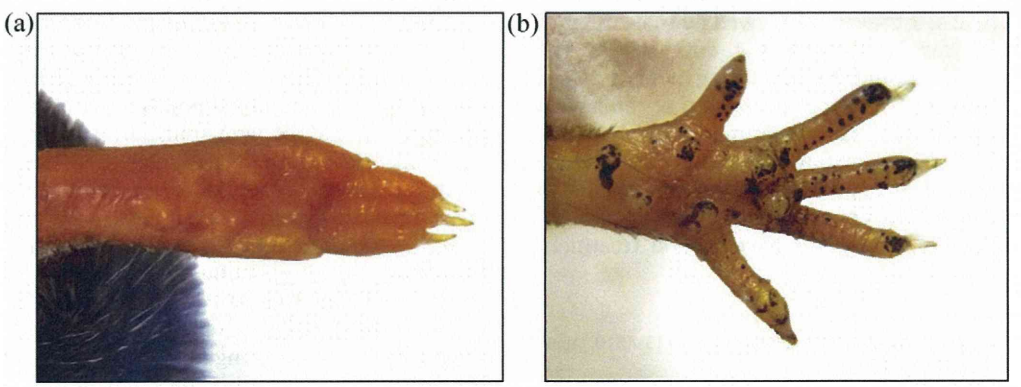

Fig. 1. Confirmation of non-sweating/sweating of mice through their paws. Representative photographs of the paw of a non-sweating/sweating mouse are shown. (a) No spot corresponding to sweat secretion was apparent on the paw of an anesthetized mouse. (b) Numerous spots were observed on the paw of a mouse which was held in the hand without anesthesia.

3. Results

3.1. AQP5 translocated from the non-apical region to the apical membranes in cells of mouse sweat glands under sweating condition

AQP5 was reported to translocate to the apical membranes of cells of rat parotid glands with cevimeline, a muscarinic receptor agonist [15]. We therefore assessed changes in the subcellular localization of AQP5 in sweat glands during sweating in mice. To determine whether the mice were sweating or not through their paws, we used a modified Minor method. In the control anesthetized mice, spots which correspond to sweat secretion, were scarcely observed on the paws (Fig. 1a). To make the mice sweat, we chose to simply hold the mice in our hands without anesthesia, rather than to apply a sweating agent such as pilocarpine or acetylcholine, since more spots were observed on the paws of the held mice than the mice given sweating agents (Fig. S1). After confirming that the mice were in non-sweating or sweating condition, the paws were removed and processed for immunofluorescence. Under non-sweating condition, AQP5 was detected in the apical membranes of secretory cells in the mouse sweat glands, and was diffusely localized in the non-apical region

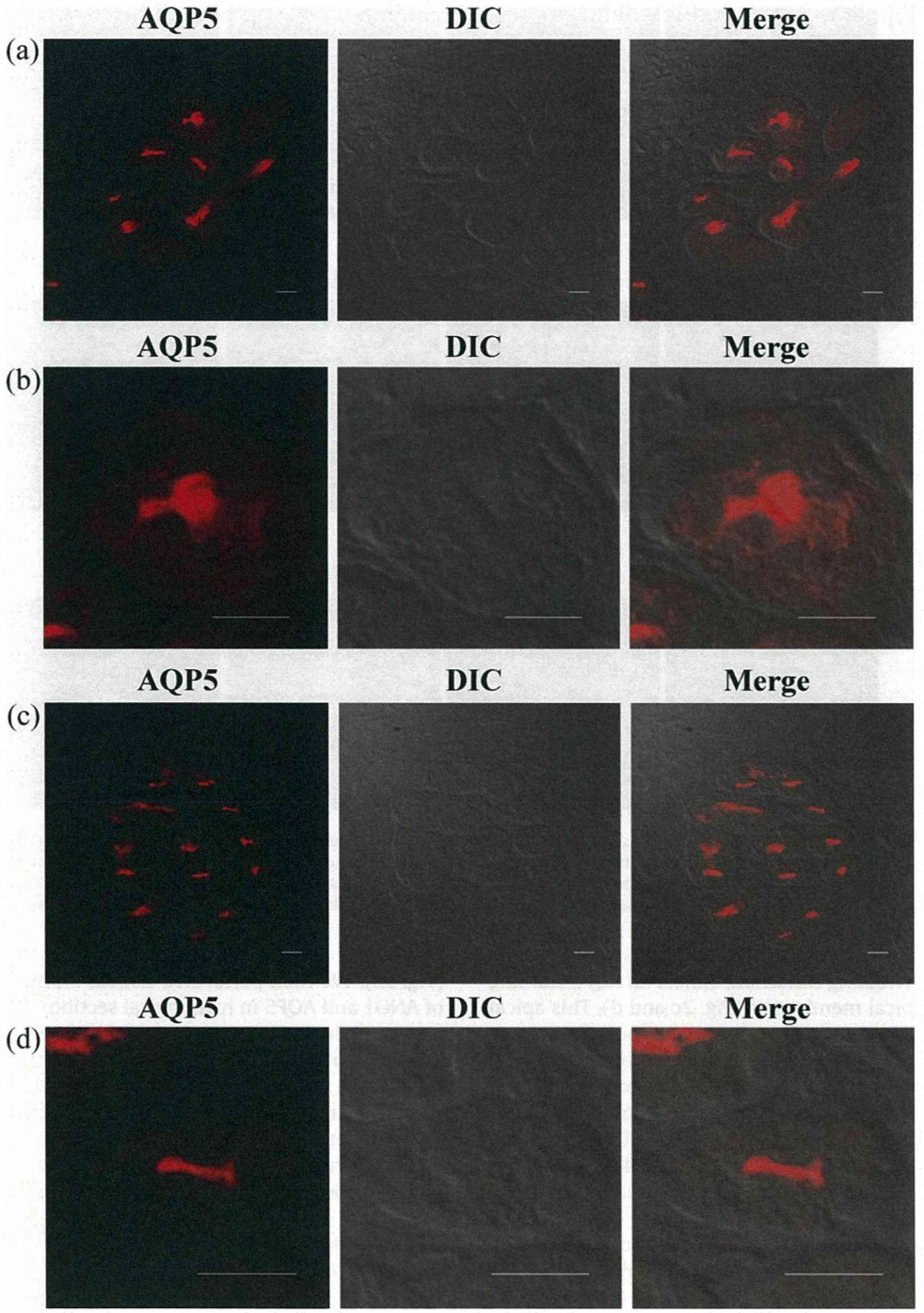

Fig. 2. Aquaporin-5 (AQP5) translocation from the non-apical region to the apical membranes of cells in mouse sweat glands. (a–d) Immunofluorescent staining of AQP5 localization in paraffin sections of a representative mouse sweat gland under non-sweating or sweating conditions. (a and b) Under non-sweating condition, immunoreactive AQP5 was detected in the apical membranes as well as in the non-apical region of the secretory cells. (c and d) Under sweating condition, almost all immunoreactive AQP5 was detected in the apical membranes. Bar = 10 μm.

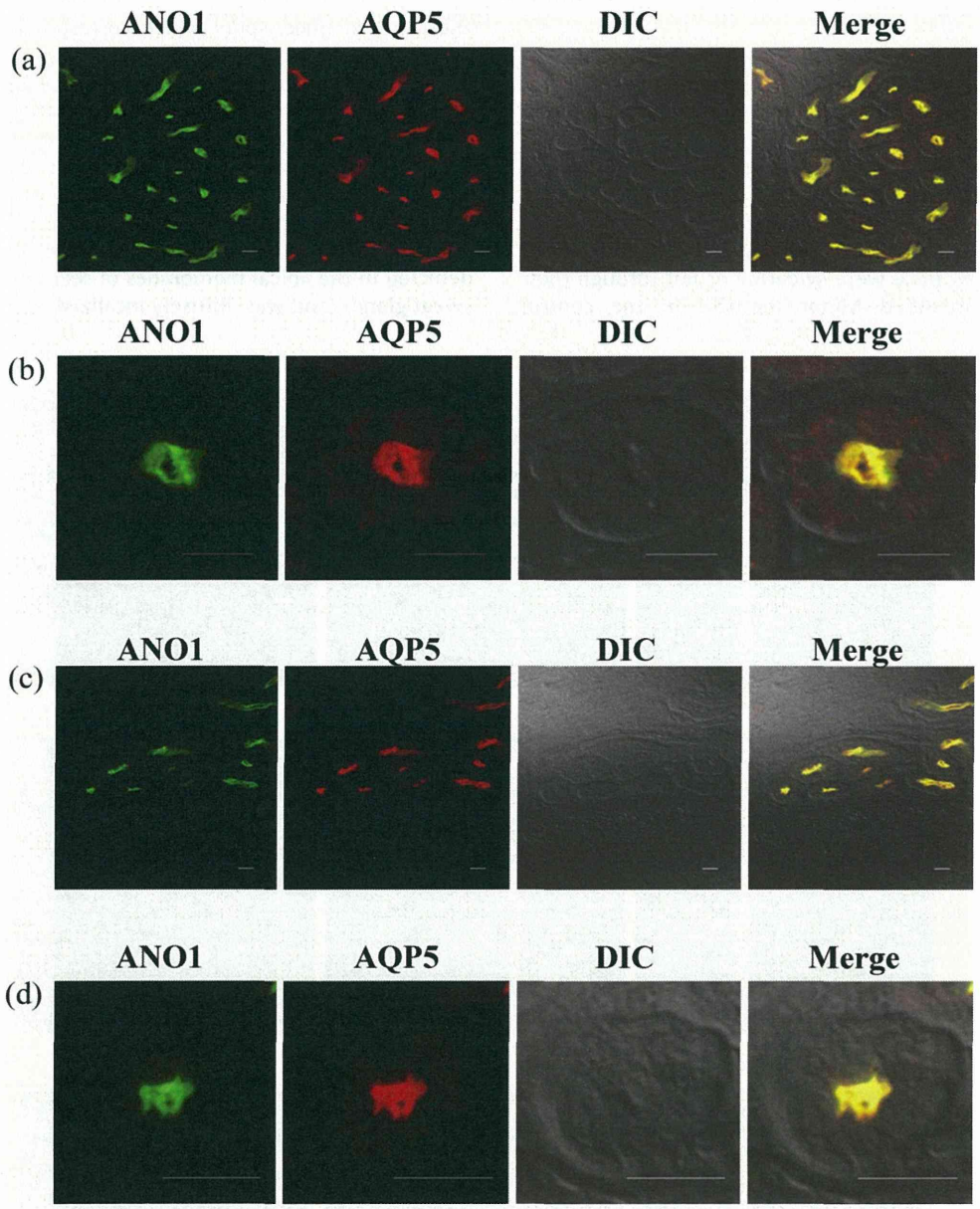

Fig. 3. Colocalization of anoctamin-1 (ANO1) and AQP5 in mouse sweat glands. Double immunofluorescent staining of ANO1 (green) and AQP5 (red) in histological sections of the paw of a representative mouse under non-sweating or sweating condition are shown. (a and b) Under non-sweating condition, immunoreactive ANO1 was detected in the apical membranes of the secretory cells and partially colocalized with AQP5. (c and d) Under sweating condition, immunoreactive ANO1 was detected in the apical membranes of these cells and colocalized with AQP5 in the apical membranes. The cellular localization of ANO1 did not change during sweating. Bar = 10 μm.

(Fig. 2a and b). Under sweating condition, almost all AQP5 staining was detected in the apical membranes (Fig. 2c and d). This apical accumulation of AQP5 was also confirmed in the pilocarpine-induced sweating (Fig. S1). The fluorescent intensity in the apical AQP5 in the cross section of the coils was significantly increased from 60 ± 7.7% (n = 15) under non-sweating condition to 91 ± 6.0% (n = 15) under sweating condition (mean ± SD, $P < 0.01$). These data suggested that a certain amount of AQP5 translocated from the non-apical region to the apical membranes during sweating.

Supplementary material related to this article found, in the online version, at http://dx.doi.org/10.1016/j.jdermsci.2013.01.013.

To exclude the possibility that translocation of AQP5 to the apical membranes is a general characteristic of apical membrane proteins in sweat glands during sweating, we investigated the localization of anoctamin-1 (ANO1), a calcium-activated chloride channel [16–18], during sweating. ANO1 immunofluorescence was detected in the apical membranes of cells in mouse sweat glands (Fig. S2). We then performed double immunofluorescent analysis of ANO1 and AQP5 in histological sections of the mice paws under non-sweating and sweating conditions. ANO1 was detected only in the apical membranes under both conditions, and it completely colocalized with AQP5 in these apical membranes (Fig. 3). However, in contrast to AQP5, the localization of ANO1 did not differ under the different applied conditions.

Supplementary material related to this article found, in the online version, at http://dx.doi.org/10.1016/j.jdermsci.2013.01.013.

3.2. Immunohistochemical analysis of AQP5 localization in human eccrine sweat glands

To determine the cellular localization of AQP5 in human eccrine sweat glands, we immunohistochemically analyzed paraffin sections of healthy human skin using the anti-AQP5 antibody. In addition, the anti-Na^+/K^+ATPase antibody was used for visualizing

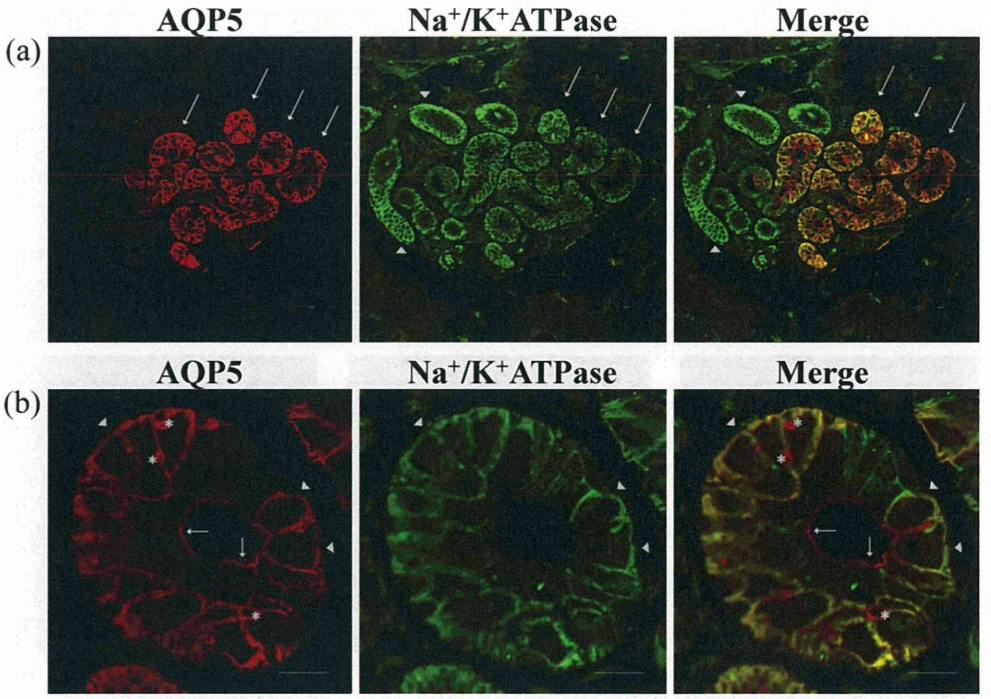

Fig. 4. Immunohistochemical analysis of AQP5 localization in human eccrine sweat glands. (a) Representative double immunofluorescent staining of AQP5 (red) and Na^+/K^+ATPase (green) in a paraffin section of a human eccrine sweat gland. Immunoreactive AQP5 was detected in cells of the secretory portion of the gland (arrows), but not in duct cells (arrowheads). (b) Close up images of the secretary coil of a human eccrine sweat gland. Immunoreactive AQP5 was detected in the apical membranes (arrows) and in the intercellular canaliculi (asterisks), and did not colocalize with Na^+/K^+ATPase in these areas. AQP5 was also detected in the basolateral membranes of the clear cells (arrowheads) where it did colocalize with Na^+/K^+ATPase. Bar = 10 μm.

the morphology of the eccrine sweat gland (Fig. 4). Immunoreactive AQP5 was detected in cells in the secretory portion of the eccrine sweat gland, but not in duct cells, whereas immunoreactive Na^+/K^+ATPase was detected in cells of both the secretory portion and the duct. Sweat gland duct cells showed strong Na^+/K^+ATPase labeling at their basolateral plasma membranes as previously reported [19,20], whereas cells in the secretory portion showed relatively weak labeling at their basolateral plasma membranes (Fig. 4a). AQP5 was detected in the apical membranes (Fig. 4b, arrows) of cells in the secretory portion as well as in the intercellular canaliculi (Fig. 4b, asterisks), and this AQP5 staining did not colocalize with Na^+/K^+ATPase staining. In addition, AQP5 was also detected in the basolateral membranes of the clear cells (Fig. 4b, arrowheads). Cytoplasmic staining of AQP5 as observed in mouse sweat glands was not observed in our specimens of human eccrine sweat glands. Analysis of different specimens of healthy skin from several patients using two other anti-AQP5 antibodies (sc-9890 and sc-28628, Santa Cruz Biotechnology) indicated almost exactly the same distribution of AQP5 shown in Fig. 4. AQP5 was not detected in other components of the skin, including the epidermis, sebaceous glands and hair follicles (data not shown).

3.3. Transfected human AQP5 is located at both the apical and basolateral membranes of MDCK cells

To further investigate AQP5 cellular localization and translocation, we generated MDCK cell lines stably expressing non-tagged hAQP5. The transfected hAQP5 was not tagged since some tag sequences are known to affect the cellular localization of AQP5 [21]. We selected nine clones from these transfected cells based on Western blotting of AQP5 protein expression (Fig. 5a). Of these clones, clone #6, which showed a high level of AQP5 expression, and a mixture of clones #4, #7 and #9, which was used to avoid the effect of clonal variation on the results, were selected for further experiments. In preliminary experiments, we confirmed that these cells formed a confluent monolayer and were in a polarized state by checking the basolateral localization of Na^+/K^+ATPase (data not shown). A cell-side-specific biotinylation assay showed that hAQP5 was present at both the apical and basolateral membranes of these cells (Fig. 5b), which was consistent with the immunohistochemical localization of AQP5 in human eccrine sweat glands in vivo (Fig. 4).

3.4. Human AQP5 translocated from the cytoplasm to the apical membranes by treatment with calcium ionophore

In rat parotid glands, the interaction of acetylcholine with M3 muscarinic receptors and of norepinephrine with α1-adrenergic receptors stimulates salivary secretion by inducing an elevation of intracellular calcium concentration and the translocation of rat AQP5 from the intracellular membranes to the apical membranes [22,23]. Sweating is also primarily regulated by

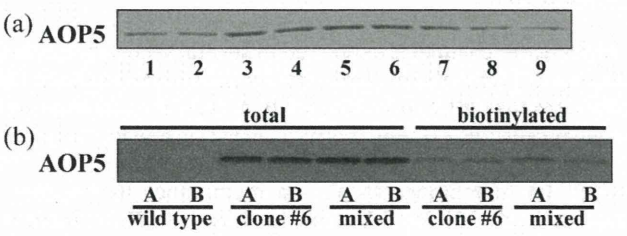

Fig. 5. Analysis of MDCK cell lines stably expressing non-tagged hAQP5. (a) Nine independent clones were isolated and their expression of hAQP5 was analyzed by Western blotting. Clone #6, which showed a high level of AQP5 expression, and a mixture of clones #4, #7 and #9, which was used to avoid the effect of clonal variation, were selected for further experiments. (b) Localization of hAQP5 in the stable cell lines was determined by a cell-side-specific biotinylation assay. The hAQP5 was detected at both the apical and basolateral sides of polarized hAQP5-MDCK cells. A, apical membrane fraction; B, basolateral membrane fraction; wild-type, wild-type MDCK cell line; mixed, mixed clone of #4, #7 and #9.

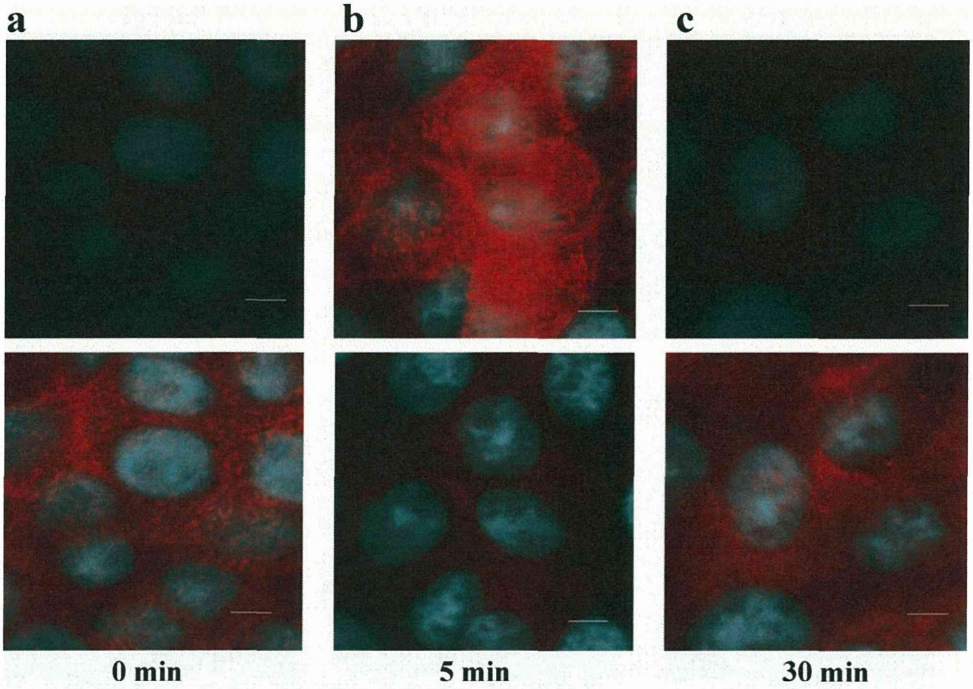

Fig. 6. Immunofluorescent analysis of human AQP5 translocation to the apical membranes of MDCK cells. Confocal images of hAQP5 in MDCK cells (clone #6) treated with 10 μM A23187. The top and bottom images show hAQP5 at the apical surface and the nucleus levels of the monolayers, respectively. hAQP5 at the apical surface level was increased 5 min after treatment. Red: AQP5, blue: 4,6-diamidino-2-phenylindole (DAPI). Bar = 5 μm.

acetylcholine, which causes an increase in intracellular calcium concentration via muscarinic receptors [1]. We therefore tried to determine whether hAQP5 translocation was regulated by an increase in intracellular calcium concentration in MDCK cells stably expressing non-tagged hAQP5. Confluent monolayers of the hAQP5-MDCK cells were treated with or without (control) 10 μM calcium ionophore A23187 for 5 or 30 min and were then subjected to an immunofluorescent analysis and a cell-side-specific biotinylation assay. In both analyses, the amount of hAQP5 protein in the apical membrane fraction increased after 5 min of A23187 treatment compared to control cells (Figs. 6 and 7a and e), and it returned to the control level 30 min after this treatment (Figs. 6 and 7b and f). On the other hand, the amount of hAQP5 protein in the basolateral membrane fraction did not change at either 5 or 30 min after treatment (Fig. 7c, d, g and h). The same results were obtained using 20 μM thapsigargin, another reagent that increases intracellular calcium concentration (data not shown). These results suggest that hAQP5 protein translocated relatively rapidly from the cytoplasm to the apical membranes due to an increase in intracellular calcium.

4. Discussion

AQP5 water channel is expressed in several secretory epithelia, including salivary glands [24], airway submucosal glands [25], lacrimal glands [26], and sweat glands, as well as in alveolar type I epithelial cells [25,27]. Aquaporin-2 (AQP2) is a water channel in the collecting ducts of the kidney that translocates from intracellular membranes to plasma membranes in response to vasopressin [28–30]. AQP5 has 63% identity to AQP2 [31], and was shown to translocate from the cytoplasm to the apical membranes in cells of rat salivary glands by stimulation with M3 muscarinic and α1-adrenergic agonists [22,23]. However, there has been no report regarding AQP5 translocation in cells of sweat glands. Since it was difficult to investigate the mechanism of AQP5 translocation in human tissues, we first used mouse tissues for this investigation. We observed the significant decrease of mouse AQP5 in the non-apical region and its accumulation in the apical membranes under sweating condition (Fig. 2). This is the first report of AQP5 translocation in sweat glands in vivo.

In human samples, however, we could not observe apparent cytoplasmic AQP5 signals (Fig. 4). We speculate that the patients undergoing biopsy were under emotional sweating condition due to mental strain. To verify this speculation, the specimen of anhidrotic skin, for example, skin from the patients who had underwent sympathectomy, may be necessary.

We consider that apical translocation is not a general characteristic of apical membrane proteins involved in sweating since we could not observe the translocation of ANO1 in the same sections (Fig. 3). ANO1 is the first member of a family of calcium-activated chloride channels that were recently identified as anoctamins [16–18]. Although calcium-activated chloride channels have been postulated to be involved in sweating, the presence of anoctamins in sweat glands has not been reported. We believe that this is the first report to clearly demonstrate ANO1 apical membrane localization in sweat glands and to show that ANO1 does not translocate during sweating. Since the function of ANO1 is regulated by calcium, it is reasonable to presume that ANO1 does not need to traffic within the cell for its function. Thus, the findings of the present study, i.e., that AQP5 colocalizes with ANO1 in sweat glands, and that AQP5 translocates during sweating, provide new insights into the mechanism by which primary sweat is produced.

We could detect human AQP5 signals in the basolateral membranes as well as in the apical membranes (Fig. 4). There must be high water permeability in both apical and basolateral plasma membranes for tight epithelia to be highly permeable to water. In kidney collecting ducts, there are AQP3 and AQP4 in the basolateral plasma membranes, which make the membranes constitutively permeable to water. The trafficking of AQP2 to the apical membranes is the key machinery to increase transepithelial water permeability by vasopressin signal. We speculate that basolateral AQP5 in sweat glands may have the same role as AQP3 and AQP4 in the collecting ducts.

The principal regulator of sweat secretion in primates and rodents is acetylcholine [1,32], whose effects are mediated by the

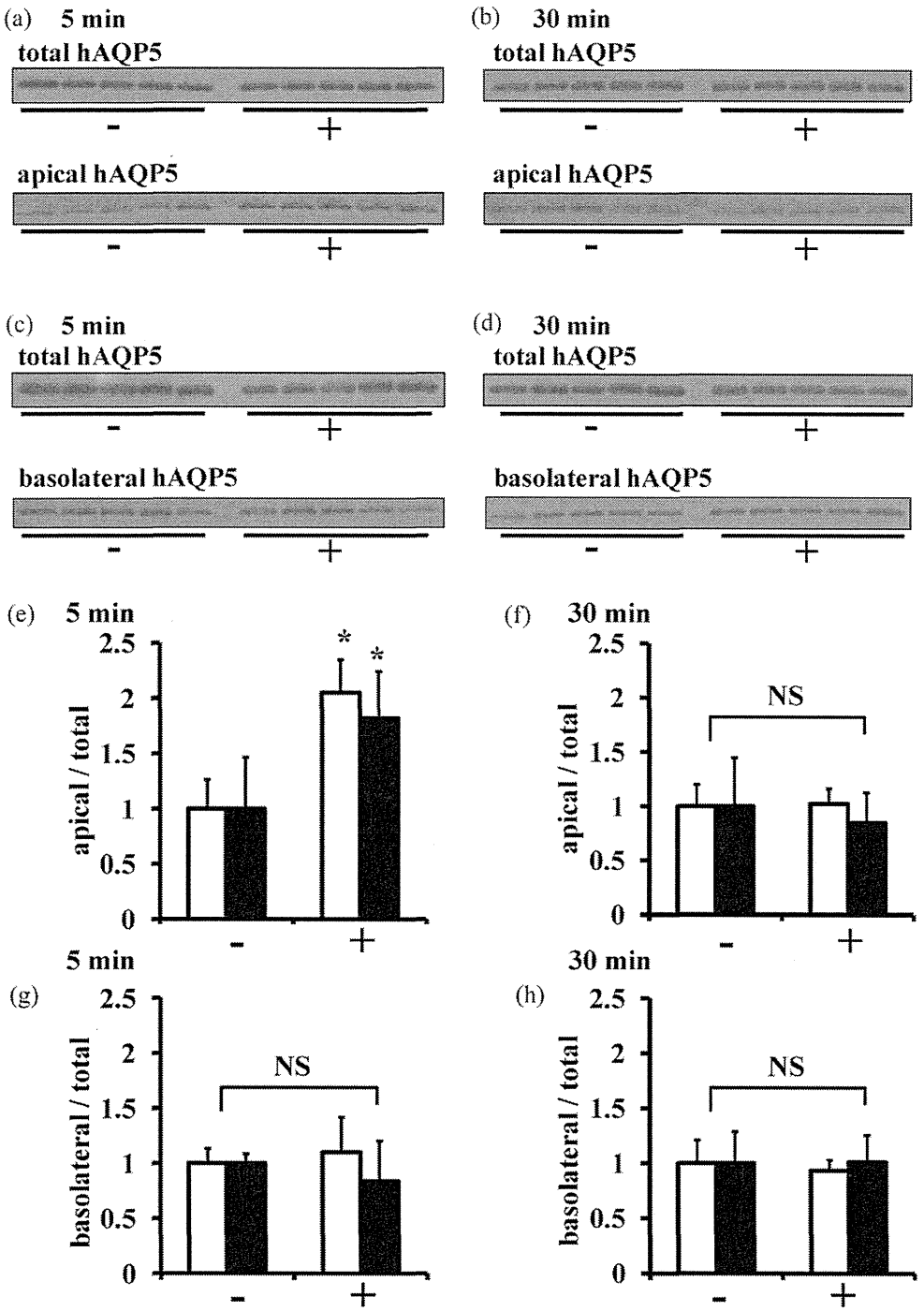

Fig. 7. Human AQP5 translocation from the cytoplasm to the apical membranes of MDCK cells. (a–d) Confluent monolayers of the hAQP5-MDCK cells were treated with or without (control) 10 μM calcium ionophore A23187 and then subjected to a cell-side-specific biotinylation assay. The figures are representative results using clone #6. (e–h) Densitometric analysis of (a–d) and the results using mixed clone. After 5 min of the treatment (a and e), the apical hAQP5 level increased by about twofold in A23187-treated cells, and after 30 min of the treatment (b and f), it returned to the control level. The basolateral hAQP5 level did not change after 5 or 30 min of the treatment (c, d, g, h). White bars, clone #6 ($n = 5$); black bars, mixed clone ($n = 5$). Error bars indicate SD. *$P < 0.05$. NS; not significant.

intracellular second messenger calcium. We therefore tried to determine if human AQP5 translocation was mediated by intracellular calcium using a cell culture system. The signaling pathways that are involved in AQP5 trafficking in vitro have been investigated using several types of epithelial cells. Biochemical analysis of slices of rat parotid glands suggested that AQP5 is translocated from cytoplasmic compartments to the apical membrane fraction by stimulation of M3 muscarinic receptors and α1-adrenergic receptors [22,23]. Rat AQP5 in human salivary gland (HSG) cells was shown to undergo rapid translocation to plasma membranes by treatment with thapsigargin, an inhibitor of the endoplasmic Ca^{2+}ATPase or with calcium ionophore A23187 [33]. However, this study was not performed in the cells under polarized condition, and the translocation evaluated only by immunofluorescence appeared to be localized not to the apical but to the lateral plasma membranes [33]. Unlike rat AQP5 in parotid glands, human AQP5 is present both in the apical and basolateral plasma membranes in sweat glands (Fig. 4). Therefore, we thought that we should determine the translocation of human AQP5 in polarized cells. In addition, we used non-tagged AQP5 for our study since a previous report indicated that

the cellular behavior of AQP5, especially in terms of membrane trafficking in cell culture systems, appears to be significantly influenced by tag sequences attached to AQP5 [21]. Although we would have liked to perform this experiment in cells derived from an eccrine sweat gland, there is no such cells feasible for this type of experiment, so we used MDCK cells instead. MDCK cells form a polarized epithelial monolayer when grown on a permeable support [34,35], and have been one of the most useful model cells for the study of intracellular trafficking of molecules in epithelial cells.

hAQP5 localized both apically and basolaterally in all isolated stable clones of hAQP5-transfected MDCK cells with a similar pattern as that of AQP5 in human eccrine sweat glands in vivo. The observed behavior of non-tagged human AQP5 in these cell lines, i.e., rapid translocation only to the apical plasma membrane by A23187 and thapsigargin treatment, is also consistent with the translocation observed in vivo, clearly suggesting that intracellular calcium is an important regulator of apical AQP5 trafficking in sweating. At present, little is known about the molecular mechanism(s) of AQP5 trafficking by intracellular calcium. Unlike AQP2, whether AQP5 phosphorylation is involved in the mechanism(s) remains to be determined.

Regarding the role of AQP5 in sweat glands, the previous knockout mouse studies reported contradictory results: one study demonstrated dramatically reduced sweating in AQP5 null (−/−) mice [12], while the other study demonstrated no significant difference in sweating between wild-type mice and AQP5 null (−/−) mice [11]. The reason for this discrepancy is not clear at present. Our study clearly showed the existence of regulated apical translocation of AQP5 in sweat glands, which does not answer whether AQP5 is necessary for sweating or not, but suggests that AQP5 may contribute to sweat secretion by increasing the water permeability of apical plasma membranes of sweat glands.

In conclusion, we clearly demonstrated the rapid translocation of AQP5 to the apical plasma membranes during sweating and by the agents increasing intracellular calcium concentration. Agents that modulate AQP5 function may be useful for the treatment of patients with sweating disorders.

Funding sources

This study was supported by Health and Labor Sciences Research Grants from Ministry of Health, Labor and Welfare of Japan: Research on intractable diseases (Nos. 0309001, 1211202), Grant-in-Aid for Scientific Research (A) from the Japan Society for the Promotion of Science (Nos. 20249047, 22249032), Takeda Science Foundation, and Salt Science Research Foundation (1026).

Acknowledgments

We thank Chiyako Miyagishi and Motoko Chiga of Tokyo Medical and Dental University for excellent technical assistance.

References

[1] Sato K. The physiology, pharmacology, and biochemistry of the eccrine sweat gland. Rev Physiol Biochem Pharmacol 1997;79:51–131.
[2] Dobson RL, Sato K. The secretion of salt and water by the eccrine sweat gland. Arch Dermatol 1972;105:366–70.
[3] Swartling C, Naver H, Lindberg M. Botulinum A toxin improves life quality in severe primary focal hyperhidrosis. Eur J Neurol 2001;8:247–52.
[4] Cinà CS, Clase CM. The illness intrusiveness rating scale: a measure of severity in individuals with hyperhidrosis. Qual Life Res 1999;8:693–8.
[5] Hornberger J, Grimes K, Naumann M, Glaser DA, Lowe NJ, Naver H, et al. Multispecialty working group on the recognition, and treatment of primary focal hyperhidrosis, recognition, diagnosis, and treatment of primary focal hyperhidrosis. J Am Acad Dermatol 2004;51:274–86.
[6] Doolabh N, Horswell S, Williams M, Huber L, Prince S, Meyer DM, et al. Thoracoscopic sympathectomy for hyperhidrosis: indications and results. Ann Thorac Surg 2004;77:410–4 [discussion 414].
[7] Ishibashi K, Hara S, Kondo S. Aquaporin water channels in mammals. Clin Exp Nephrol 2009;13:107–17.
[8] Ma L, Huang YG, He H, Deng YC, Zhang HF, Che HL, et al. Postnatal expression and denervation induced up-regulation of aquaporin-5 protein in rat sweat gland. Cell Tissue Res 2007;329:25–33.
[9] Ma L, Huang YG, Deng YC, Tian JY, Rao ZR, Che HL, et al. Topiramate reduced sweat secretion and aquaporin-5 expression in sweat glands of mice. Life Sci 2007;80:2461–8.
[10] Kabashima K, Shimauchi T, Kobayashi M, Fukamachi S, Kawakami C, Ogata M, et al. Aberrant aquaporin 5 expression in the sweat gland in aquagenic wrinkling of the palms. J Am Acad Dermatol 2008;59:S28–32.
[11] Song Y, Sonawane N, Verkman AS. Localization of aquaporin-5 in sweat glands and functional analysis using knockout mice. J Physiol 2002;541:561–8.
[12] Nejsum LN, Kwon TH, Jensen UB, Fumagalli O, Frøkiaer J, Krane CM, et al. Functional requirement of aquaporin-5 in plasma membranes of sweat glands. Proc Natl Acad Sci USA 2002;99:511–6.
[13] Iizuka T, Suzuki T, Nakano K, Sueki H. Immunolocalization of aquaporin-5 in normal human skin and hypohidrotic skin diseases. J Dermatol 2012;39:344–9.
[14] Yui N, Okutsu R, Sohara E, Rai T, Ohta A, Noda Y, et al. FAPP2 is required for aquaporin-2 apical sorting at trans-Golgi network in polarized MDCK cells. Am J Physiol Cell Physiol 2009;297:C1389–96.
[15] Ishikawa Y, Yuan Z, Inoue N, Skowronski MT, Nakae Y, Shono M, et al. Identification of AQP5 in lipid rafts and its translocation to apical membranes by activation of M3 mAChRs in interlobular ducts of rat parotid gland. Am J Physiol Cell Physiol 2005;289:C1303–11.
[16] Caputo A, Caci E, Ferrera L, Pedemonte N, Barsanti C, Sondo E, et al. TMEM16A, a membrane protein associated with calcium-dependent chloride channel activity. Science 2008;322:590–4.
[17] Schroeder BC, Cheng T, Jan YN, Jan LY. Expression cloning of TMEM16A as a calcium-activated chloride channel subunit. Cell 2008;134:1019–29.
[18] Yang YD, Cho H, Koo JY, Tak MH, Cho Y, Shim WS, et al. TMEM16A confers receptor-activated calcium-dependent chloride conductance. Nature 2008;455:1210–5.
[19] Quinton PM, Tormey JM. Localization of Na/K-ATPase sites in the secretory and reabsorptive epithelia of perfused eccrine sweat glands: a question to the role of the enzyme in secretion. J Memb Biol 1976;29:383–99.
[20] Saga K, Sato K. Ultrastructural localization of ouabain-sensitive, K-dependent p-nitrophenyl phosphatase activity in monkey eccrine sweat gland. J Histochem Cytochem 1988;36:1023–30.
[21] Kosugi-Tanaka C, Li X, Yao C, Akamatsu T, Kanamori N, Hosoi K. Protein kinase A-regulated membrane trafficking of a green fluorescent protein-aquaporin 5 chimera in MDCK cells. Biochim Biophys Acta 2006;1763:337–44.
[22] Ishikawa Y, Eguchi T, Skowronski MT, Ishida H. Acetylcholine acts on M3 muscarinic receptors and induces the translocation of aquaporin5 water channel via cytosolic Ca^{2+} elevation in rat parotid glands. Biochem Biophys Res Commun 1998;245:835–40.
[23] Ishikawa Y, Skowronski MT, Inoue N, Ishida H. alpha(1)-adrenoceptor-induced trafficking of aquaporin-5 to the apical plasma membrane of rat parotid cells. Biochem Biophys Res Commun 1999;265:94–100.
[24] Ma T, Song Y, Gillespie A, Carlson EJ, Epstein CJ, Verkman AS. Defective secretion of saliva in transgenic mice lacking aquaporin-5 water channels. J Biol Chem 1999;274:20071–74.
[25] Nielsen S, King LS, Christensen BM, Agre P. Aquaporins in complex tissues. II. Subcellular distribution in respiratory and glandular tissues of rat. Am J Physiol 1997;273:C1549–61.
[26] Moore M, Ma T, Yang B, Verkman AS. Tear secretion by lacrimal glands in transgenic mice lacking water channels AQP1, AQP3, AQP4 and AQP5. Exp Eye Res 2000;70:557–62.
[27] Dobbs LG, Gonzalez R, Matthay MA, Carter EP, Allen L, Verkman AS. Highly water-permeable type I alveolar epithelial cells confer high water permeability between the airspace and vasculature in rat lung. Proc Natl Acad Sci USA 1998;95:2991–6.
[28] Yamamoto T, Sasaki S, Fushimi K, Ishibashi K, Yaoita E, Kawasaki K. Vasopressin increases AQP-CD water channel in apical membrane of collecting duct cells in Brattleboro rats. Am J Physiol 1995;268:C1546–51.
[29] Nielsen S, DiGiovanni SR, Christensen EI, Knepper MA, Harris HW. Cellular and subcellular immunolocalization of vasopressin-regulated water channel in rat kidney. Proc Natl Acad Sci USA 1993;90:11663–67.
[30] Fushimi K, Uchida S, Hara Y, Hirata Y, Marumo F, Sasaki S. Cloning and expression of apical membrane water channel of rat kidney collecting tubule. Nature 1993;361:549–52.
[31] Raina S, Preston GM, Guggino WB, Agre P. Molecular cloning and characterization of an aquaporin cDNA from salivary, lacrimal, and respiratory tissues. J Biol Chem 1995;270:1908–12.
[32] Sato K, Cavallin S, Sato KT, Sato F. Secretion of ions and pharmacological responsiveness in the mouse paw sweat gland. Clin Sci (Lond) 1994;86:133–9.
[33] Tada J, Sawa T, Yamanaka N, Shono M, Akamatsu T, Tsumura K, et al. Involvement of vesicle–cytoskeleton interaction in AQP5 trafficking in AQP5-gene-transfected HSG cells. Biochem Biophys Res Commun 1999;266:443–7.
[34] Cereijido M, Robbins ES, Dolan WJ, Rotunno CA, Sabatini DD. Polarized monolayers formed by epithelial cells on a permeable and translucent support. J Cell Biol 1978;77:853–80.
[35] Misfeldt DS, Hamamoto ST, Pitelka DR. Transepithelial transport in cell culture. Proc Natl Acad Sci USA 1976;73:1212–6.

THE JOURNAL OF DERMATOLOGY

doi: 10.1111/1346-8138.12099

Journal of Dermatology 2013; **40**: 344–354

GUIDELINE

Guidelines for the diagnosis and treatment of vitiligo in Japan

Naoki OISO,[1] Tamio SUZUKI,[2] Mari WATAYA-KANEDA,[3] Atsushi TANEMURA,[3] Miki TANIOKA,[4] Tomoko FUJIMOTO,[5] Kazuyoshi FUKAI,[6] Tamihiro KAWAKAMI,[7] Katsuhiko TSUKAMOTO,[8] Yuji YAMAGUCHI,[9] Shigetoshi SANO,[10] Yoshihiko MITSUHASHI,[11] Chikako NISHIGORI,[12] Akimichi MORITA,[13] Hidemi NAKAGAWA,[14] Masako MIZOGUCHI,[7] Ichiro KATAYAMA[3]

[1]Department of Dermatology, Kinki University Faculty of Medicine, Osaka-Sayama, [2]Department of Dermatology, Yamagata University Faculty of Medicine, Yamagata, [3]Department of Dermatology Integrated Medicine, Osaka University Graduate School of Medicine, Suita, [4]Department of Dermatology, Kyoto University Graduate School of Medicine, Kyoto, [5]Department of Dermatology, Tokyo Medical and Dental University, Tokyo, [6]Department of Dermatology, Osaka City University Graduate School of Medicine, Osaka, [7]Department of Dermatology, St Marianna University School of Medicine, Kawasaki, [8]Department of Dermatology, Yamanashi Prefectural Central Hospital, Kofu, [9]Abbott Japan, [10]Department of Dermatology, Kochi Medical School, Kochi University, Kochi, [11]Department of Dermatology, Tokyo Medical University Dermatology Clinic, Tokyo, [12]Division of Dermatology, Department of Internal Related, Faculty of Medicine, Kobe University Graduate School of Medicine, Kobe, [13]Department of Geriatric and Environmental Dermatology, Nagoya City University Graduate School of Medical Sciences, Nagoya, and [14]Department of Dermatology, The Jikei University School of Medicine, Tokyo, Japan

ABSTRACT

Vitiligo is an acquired pigment disorder in which depigmented macules result from the loss of melanocytes from the involved regions of skin and hair. The color dissimilarity on the cosmetically sensitive regions frequently induces quality of life impairment and high willingness to pay for treatment in patients with vitiligo. The Vitiligo Japanese Task Force was organized to overcome this situation and to cooperate with the Vitiligo Global Issues Consensus Conference. This guideline for the diagnosis and treatment of vitiligo in Japan is proposed to improve the circumstances of Japanese individuals with vitiligo. Its contents include information regarding the diagnosis, pathogenesis, evaluation of disease severity and effectiveness of treatment, and evidence-based recommendations for the treatment of vitiligo. The therapeutic algorithm based on the proposed recommendation is designed to cure and improve the affected lesions and quality of life of individuals with vitiligo.

Key words: **algorithm, diagnosis, guideline, phototherapy, vitamin D_3 analogs, vitiligo.**

INTRODUCTION

Vitiligo is the most common acquired depigmented disorder characterized by the progressive loss of melanocytes. It is mainly classified into segmental and non-segmental vitiligo. The color dissimilarity of the cosmetically sensitive regions is associated with significant burden, as reflected by the quality of life (QOL) impairment and high willingness to pay for treatment, especially in women.[1] A strategic guideline for the treatment of vitiligo with evidence-based evaluation has not been established.[2] Recently, novel therapies such as topical application of vitamin D_3 analogs and narrowband ultraviolet B (NB-UVB) have become more common. Thus, a guideline for the diagnosis and treatment of vitiligo in Japan would be indispensable for Japanese dermatologists making decisions regarding the management of vitiligo.

BACKGROUND OF THE GUIDELINE

The Vitiligo Japanese Task Force (VJTF) was organized for the proposition of the guideline for the diagnosis and the treatment of vitiligo in cooperation with the Japanese Dermatology Association (JDA) in October 2009.[3] The guideline was published in the Japanese published work in July 2012.[4] This English version was designed as a brief review to announce its content to scientists, physicians and dermatologists world-

Correspondence: Tamio Suzuki, M.D., Ph.D., Department of Dermatology, Yamagata University Faculty of Medicine, Iida-Nishi 2-2-2, Yamagata 990-9585, Japan. Email: tamsuz@med.id.yamagata-u.ac.jp

Conflict of interest: The authors involved in each clinical trial were excluded from being members of the committee for judging the level of evidence and the recommendation for the respective clinical trial.

Received 19 December 2012; accepted 20 December 2012.

wide. The members of the VJTF participated in the Vitiligo Global Issues Consensus Conference to cooperate with an update of the uniform concept of vitiligo and its treatment strategy.

LIMITATION OF THE GUIDELINE

This guideline was proposed following an evaluation of the established and published evidence. A forthcoming update is essential, as novel treatment may overcome current management recommendation and unexpected adverse reactions may occur in the future. The VJTF states no guarantee of protection for physicians and dermatologists against any conflict, although physicians and dermatologists insist that they refer to and follow this guideline. Dermatologists are free to manage vitiligo with strategies that are not recommended in this guideline. Therefore, the VJTF states no guarantee of protection for patients and their agents against any conflict, although patients and their agents insist that physicians and dermatologists do not refer to and do not follow this guideline. This guideline does not represent law or legal advice.

EVIDENCE LEVEL AND RECOMMENDATION

Each evidence level and recommendation was decided as described in the instructions of the guidelines for management of skin cancer (Table 1).[5]

Table 1. Criteria for levels of evidence and grades of recommendation

A. Levels of evidence
- I. Systematic review or meta-analyses
- II. One or more randomized controlled trial(s)
- III. Controlled study without randomization
- IV. Analytical epidemiological studies (cohort studies and/or case–control studies)
- V. Descriptive studies (case reports and/or case accumulation studies)
- VI. Expert committee reports or opinions from each specialist

B. Grades of recommendation
- A. Strongly recommended to perform (there should be at least one level I or II study that indicates effectiveness)
- B. Recommended to perform (there should be at least one level II study of low quality, level III of good of quality or level IV of extremely good quality that indicates effectiveness)
- C1. Can be considered for use, but there is insufficient evidence (level III–IV evidence of low quality, plural level V of good quality or level IV approved by the committee)
- C2. Not recommended for use because there is no evidence (*there is no evidence that indicates effectiveness or* there is evidence that indicates no effects)
- D. Recommended to avoid (there is good evidence that indicates no effect or harmful effects)

This table was cited from Saida *et al.*[5] with modification.

EPIDEMIOLOGY

We classified congenital and acquired depigmented disorders as shown in Figures 1 and 2, and sent a questionnaire to 262 major hospitals including all universities and medical colleges in Japan. Their replies are summarized in Figure 3. The number of patients with congenital depigmented disorders diagnosed at their first medical examination were 1748 of 912 986, and 6359 patients had acquired depigmented disorders.[3] This response demonstrated that vitiligo accounted for approximately 60% of all depigmented disorders.[1] An epidemiological survey conducted by the JDA found that patients with vitiligo comprised 1134 (the 18th most prevalent disorder in the dermatological field in Japan) of 67 488 persons who had received their first medical examination during the predetermined days in each season.[6]

CLASSIFICATION AND PATHOGENESIS OF VITILIGO

Vitiligo is a common acquired depigmented disorder, with a prevalence of approximately 0.5–1.0% in most populations.[7,8] The segmental and non-segmental forms are believed to be caused by different pathogenic mechanisms (Table 2). Genetic and environmental factors are involved in the occurrence of non-segmental vitiligo. The presence of familial vitiligo in 20–30% of vitiligo cases suggests genetic susceptibility to this disorder.[9–11] Vitiligo patients show a strong epidemiological association with several other autoimmune diseases, particularly autoimmune thyroid disease, type 1 diabetes mellitus and pernicious anemia. Blood serum examinations in patients with vitiligo show higher percentage of positive autoantibodies such as anti-thyroglobulin and anti-peroxidase antibodies. These indicate that vitiligo is mainly caused by the autoimmune loss of melanocytes in the involved areas.

With a genome-wide association study, Spritz and colleagues showed that the *NALP1* region was associated with the risk of vitiligo and several epidemiologically vitiligo-associated autoimmune and autoinflammatory diseases in Caucasians.[12] Subsequent genome-wide association studies and meta-analyses have identified multiple loci. The susceptible genes are classified into autoantigens expressing in the melanocytes, innate immunity, acquired immunity, and other function and miscellaneous.

The involvement of humoral immunity in vitiligo has been demonstrated by the presence of autoantibodies that react to a variety of melanocyte-expressed proteins such as tyrosinase, tyrosinase-related protein 1 and tyrosinase-related protein 2.[13,14] These autoantibodies induce damage to melanocytes via complement-dependent cytotoxicity and/or antibody-dependent cellular cytotoxicity. The contribution of cell-mediated immunity has been shown by the presence of human leukocyte antigen A (HLA-A)*0201 restricted, melanocyte-specific $CD8^+$ T lymphocytes in peripheral blood cells[15] and the infiltration of $CD8^+$ effector lymphocytes in the dermis. Autoimmunity is believed to be the primary mechanism of vitiligo pathogenesis. Another hypothesis includes epidermal oxidative stress.[16,17] The genesis of segmental vitiligo has not been elu-

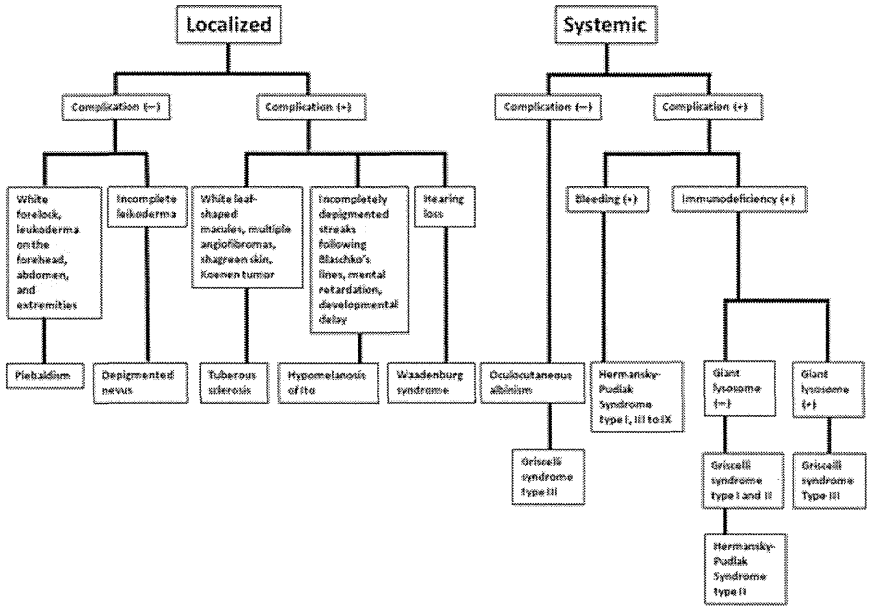

Figure 1. Classification of the congenital depigmented disorders of localized leukoderma and systemic albinism.

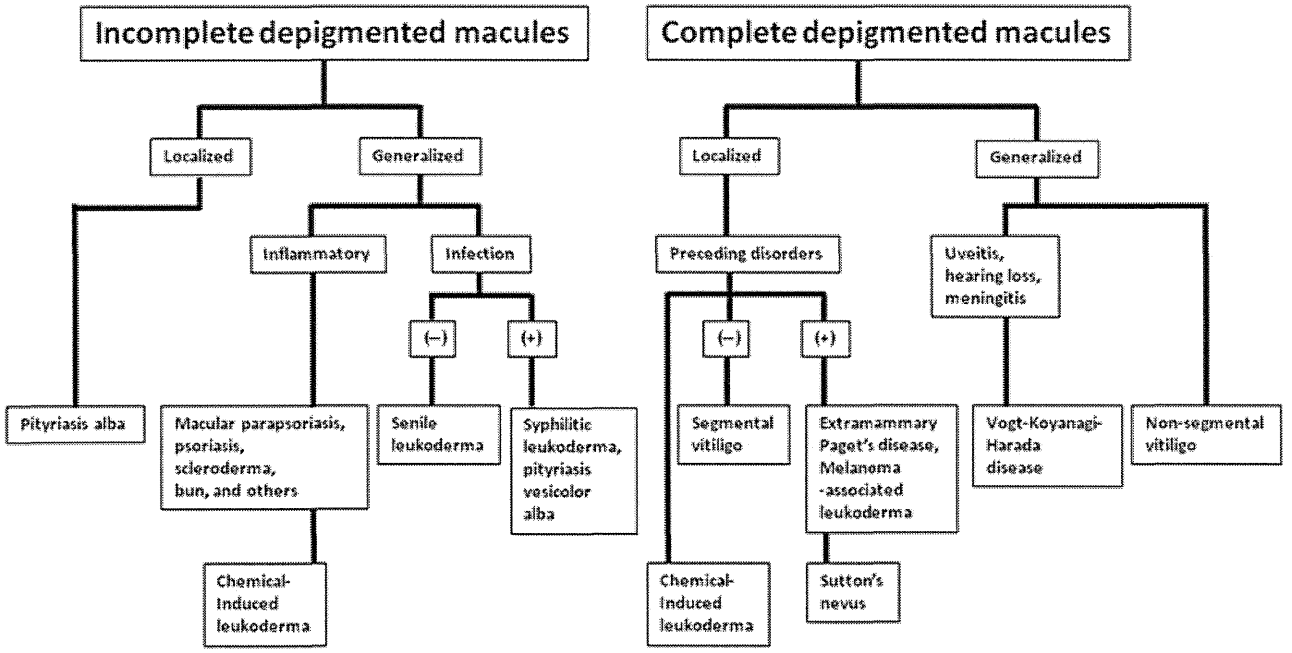

Figure 2. Classification of acquired incomplete and complete depigmented disorders.

cidated completely, despite the demonstration of elevated neuropeptide Y levels in the affected lesions.[18,19]

DIFFERENTIAL DIAGNOSIS

Vogt–Koyanagi–Harada disease

Vogt–Koyanagi–Harada (VKH) disease is a systemic disorder that affects the eyes, meninges, ears, skin and hair.[20] It is characterized by depigmentation of the affected tissues showing vitiligo, poliosis, and the sunset-glow fundus of the eyes in the late stage of the disease.[20] VKH is strongly believed to be caused by autoimmunity against melanocytes and melanin-producing cells.[20] In VKH, tyrosinase and gp100 (PMEL17) peptide-specific T-helper type 1 lymphocytes mediate an inflammatory response via producing regulated and normal T-cell expressed and secreted (RANTES),

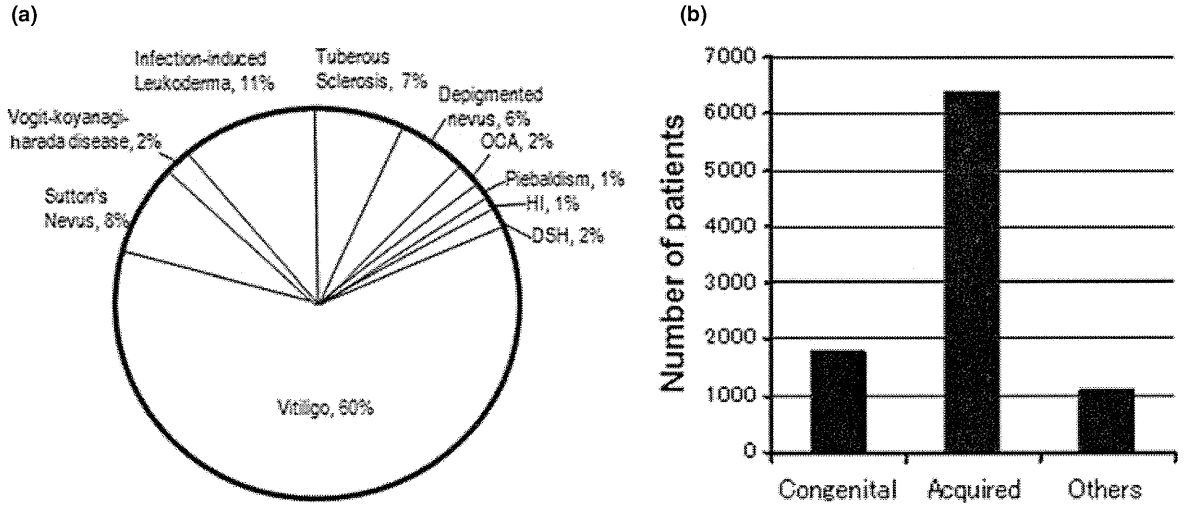

Figure 3. (a,b) Frequency of congenital and acquired depigmented disorders in Japan. The number of the patients at the first medical examination in 2009 was 912 986 in 262 major hospitals, including all universities and medical colleges. The patients with congenital depigmented disorders numbered 1748, and the patients with acquired depigmented disorders numbered 6359. DSH, dyschromatosis symmetrica hereditaria; HI, hypomelanosis of Ito; OCA, oculocutaneous albinism.

Table 2. Classification of vitiligo

1. Non-segmental vitiligo
This form includes mucosal, acrofacial, generalized and universal types, and some of focal type
2. Segmental vitiligo
This form includes some focal and mucosal types of vitiligo
3. Mixed vitiligo

chemokine (C-C motif) ligand 5 (CCR5) and interferon-γ (IFN-γ).

Sutton's phenomenon and Sutton's nevus

Sutton's phenomenon (halo phenomenon or leukoderma acquisitum centrifugum) is defined as the development of a halo of hypomelanosis around a central pigmented nevus, malignant melanoma or others. Sutton's nevus (halo nevus) is a specific halo around the nevus. Halo phenomenon/nevus is associated with the immunological response to the cells of the central nevi or tumors, namely, nevus or melanoma cells.

Infectious disorders

Acquired incomplete hypopigmented macules may be caused by various infectious disorders. Pityriasis versicolor, a fungal (*Malassezia furfur*) infectious disease, is manifested by discoloration (pityriasis versicolor nigra or pityriasis versicolor alba). Pityriasis versicolor alba is associated with incomplete transfer of melanosomes from melanocytes to keratinocytes[21] and inhibition of tyrosinase activity via C_9 and C_{11} dicarboxylic acids produced by *Pityrosporum* spp.[22] Syphilitic leukoderma, a distinctive feature of secondary syphilis, is characterized by rice-sized to nail-sized, small, obscurely demarcated, incompletely hypopigmented macules caused by decreased production of melanin granules.[23] Leukoderma can be seen in individuals infected by *Mycobacterium leprae* Hansen or HIV.

Pityriasis alba (pityriasis simplex facial)

Pityriasis alba is commonly present in children with atopic dermatitis and xerotic dermatitis. It may be confused by tinea corporis.

Senile leukoderma

Senile leukoderma is a feature of aging. It is caused by a decreased number of melanocytes and the subsequent reduction of melanin granules.

TREATMENT FOR VITILIGO

Current treatment for vitiligo in Japan

The replies to the questionnaire of the treatment of vitiligo from 262 major hospitals are summarized in Figure 4. Topical steroids, topical vitamin D_3 analogs and topical tacrolimus have been applied in almost all hospitals (~90%) and approximately 70% of institutes. Phototherapies are prevalent and are an evidence-based, highly effective treatment. They include not only traditional psoralen plus ultraviolet A therapy (PUVA) and broadband (BB)-UVB therapies but also developing NB-UVB and 308-nm excimer light/laser therapies. The efficacy of the combined treatments for vitiligo has been reported by many institutes. Camouflaging has been used for severe and stable vitiligo in approximately 90% of institutes. Topical bleaching agents for stable and treatment-resistant vitiligo are rarely applied in Japan, although this therapy is common in Europe and the USA.

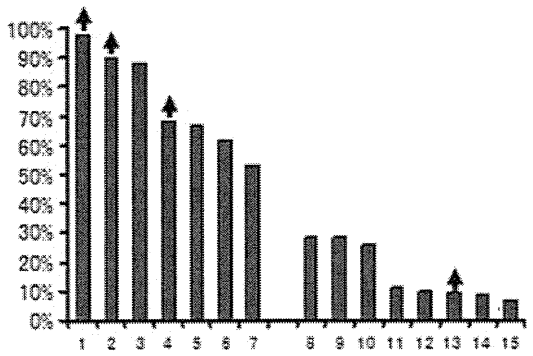

Figure 4. Situation of vitiligo treatment in 2010 in Japan. The percentages are based on the replies from 262 major hospitals, including all universities and medical colleges in Japan. (1) Topical corticosteroids; (2) camouflage; (3) topical vitamin D_3 analogs; (4) topical tacrolimus; (5) observation without any treatment; (6) narrowband ultraviolet B (NB-UVB) therapy;(7) topical psoralen and ultraviolet A (PUVA) therapy; (8) oral corticosteroids; (9) epidermal grafting; (10) mini-grafting; (11) topical bleaching agents; (12) 308-nm excimer laser/light therapy; (13) broadband (BB)-UVB therapy; and (14) abrasion. Treatments with increasing frequency of application include topical corticosteroids, camouflage, topical tacrolimus and 308-nm excimer laser/light therapy (arrows).

Evaluation of severity and treatment effectiveness in vitiligo

It is crucial to evaluate the severity of vitiligo and the efficiency of treatment. It should be discussed in global vitiligo task forces to provide uniform recommendations. Herein, we propose our theoretical explanation.

Evaluation of vitiligo severity. We proposed a classification system of vitiligo severity based on the JDA classification of atopic dermatitis severity:[24] mild, vitiligo covering less than 10% of the body surface area (BSA); moderate, vitiligo covering between 10% and 30% of the BSA; and severe, vitiligo covering more than 30% of the BSA.

Hoverer, QOL is superior to BSA. The patients with QOL impairment should be classified as those with the severe form. For example, vitiligo present on cosmetically sensitive regions with QOL impairment are classified as the severe form.[1]

Problem. This classification scheme is convenient, but it is unknown whether it is accepted by the societies for pigment cell research. It is difficult to apply this classification for evaluating the efficacy of the treatment.

Method for evaluating vitiligo severity. The Vitiligo Area Scoring Index (VASI) is recommended for the assessment of the affected surface area and the degree of depigmentation.[25] The evaluation should be performed on each area of the scalp, trunk, upper extremities and lower extremities.

Method for assessing progression and efficacy of the treatment of vitiligo. Progression and efficacy of the treatment of vitiligo can be evaluated with the VASI score. Follow-up assessments are recommended at 3 and/or 6 months after starting vitiligo treatment.

Problem. The VASI score is somewhat complicated, however, it is likely acceptable for the worldwide societies for pigment cell research. It is useful to apply the VASI score for the assessment of treatment efficacy.

Table 3. Summary of recommendations

Topical corticosteroids: A or B
Topical corticosteroids are effective for vitiligo
Topical vitamin D_3 analogs: C1–C2
Combination therapy with topical vitamin D_3 analogs and phototherapy (PUVA or NB-UVB) may be effective for vitiligo, although topical vitamin D_3 analogs alone are less efficient
Topical tacrolimus: B
Topical tacrolimus may be effective for vitiligo, although the safety of its continual use has not been established. Its effectiveness should be assessed 3 or 4 months after the initial use
Phototherapy with PUVA: B
PUVA therapy is effective for vitiligo
Phototherapy with NB-UVB: B
NB-UVB therapy is effective for adult vitiligo and is the first-line in phototherapy, as it is more effective than PUVA therapy. NB-UVB therapy is covered by Japanese public health insurance
Phototherapy with 308-nm excimer laser/light: C1
308-nm excimer laser/light therapy can be applied for vitiligo lesions in which repigmentation are expected. The features of this treatment should fully be addressed
Oral corticosteroids: C1
Oral corticosteroids can be administrated for progressing vitiligo
Immunosuppressive agents: ?
It is impossible to decide the grade of recommendation for immunosuppressive agents for the treatment of vitiligo, as only a treatment description was present[2]
Grafting and surgical treatments: A–C1
Grafting and surgical treatments should only be performed for stable and treatment-resistant vitiligo on cosmetically sensitive regions. Stability refers to no change of the affected lesions for at least more than 1 year
Camouflage: C1
Camouflage is valuable for improving QOL. Camouflage cannot cure vitiligo. Japanese health insurance does not cover camouflage

NB-UVB, narrowband ultraviolet B; PUVA, psoralen plus ultraviolet A therapy; QOL, quality of life.

Clinical questions

The briefs are summarized in Table 3.

Topical corticosteroids. Clinical question 1: Are topical corticosteroids effective for vitiligo? Recommendation: Topical corticosteroids are effective for vitiligo. Grade of recommendation: A or B.

Application of topical corticosteroids is the most prevalent treatment for vitiligo. It should be a first-line therapy for mild

or moderate vitiligo present on 10–20% of the BSA. As shown in Figure 4, almost all of the institutes use topical corticosteroids on the affected lesions. Topical application of class 2 (very strong) corticosteroids is effective, with over 75% repigmentation of localized vitiligo in 56% of cases.[26] Similarly, class 3 (strong) corticosteroid treatment is effective in 55% of cases.[26] In patients aged 15 years or below, it is suggested that class 4 (medium) corticosteroids should be applied to vitiligo lesions once a day for 4 months. In patients aged 16 years or above, it is recommended that class 2 (very strong) or class 3 (strong) corticosteroids be applied to vitiligo lesions for 4–6 months. Adverse reactions such as skin atrophy can occur due to long-term application of topical corticosteroids. No repigmentation after 2 months of topical corticosteroid treatment indicates the necessity to shift to second-line or other therapies. Repigmentation with topical corticosteroid treatment occurs in less than 20% of patients with non-segmental vitiligo.[27] Topical application of corticosteroids is not the first-line treatment of non-segmental vitiligo in adults, as phototherapy with NB-UVB is the first-line treatment.

The grade of recommendation for segmental vitiligo is A. The grade of recommendation for non-segmental vitiligo is B.

Topical vitamin D_3 analogs. Clinical question 2: Are topical vitamin D_3 analogs effective for vitiligo? Recommendation: Combined therapy with topical vitamin D_3 analogs and phototherapy (PUVA or NB-UVB) may be effective for vitiligo, although topical vitamin D_3 analogs alone are less efficient. Grade of recommendation: C1–C2.

Topical vitamin D_3 analogs are used for the treatment of vitiligo in approximately 90% of the institutes in Japan, although Japanese public health insurance does not cover this therapy. Recent reports suggest the possibility of the effectiveness of vitamin D_3 analogs.[28–30]

It has been discussed whether topical application of calcipotriol is effective for vitiligo, as the outcomes are controversial. The dissimilar results may be caused by the different reactivity of the lesions it is applied to, especially between sun-exposed and non-sun-exposed lesions. In Japan, it is forbidden to use calcipotriol on the face. The efficiency of tacalcitol hydrate and maxacalcitol for vitiligo has been reported, but they did not achieve sufficient evidence levels. At this point, a clear divergence of views emerges in the treatment of vitiligo with topical vitamin D_3 analogs.

The grade of recommendation for the treatment of vitiligo with topical vitamin D_3 analogs alone is C2. The grade of recommendation for the treatment of vitiligo with the combined therapy with topical vitamin D_3 analogs and phototherapy (PUVA or NB-UVB) is C1. Ermis *et al.*[30] showed that combination was more effective in their randomized trial. However, the examined number of the cases was not sufficient to enable an accurate evaluation. The divergent result was recently reported.

Topical tacrolimus. Clinical question 3: Is topical tacrolimus effective for vitiligo? Recommendation: Topical tacrolimus may be effective for vitiligo, although the safety of continual use has not been established. Its effectiveness should be assessed 3 or 4 months after initial use. Grade of recommendation: B.

Topical tacrolimus ointment is applied for vitiligo in approximately 70% of the institutes in Japan. Tacrolimus is the only topical calcineurin inhibitor that can be used in Japan, however, it is covered only for atopic dermatitis and not for vitiligo treatment by Japanese public health insurance. The efficiency of topical tacrolimus has been reported repeatedly over the latest decade. Once or twice daily application is effective for vitiligo. Twice daily treatment induced excellent repigmentation compared with no treatment in the same patients.[31] Hartmann *et al.*[32] reported that occlusive application enhanced the effectiveness of tacrolimus ointment in patients with vitiligo.

The grade of recommendation for the treatment of vitiligo with topical tacrolimus ointment is B. Combination therapy with topical tacrolimus and phototherapy has been examined in at least one placebo-controlled prospective trial. Although this combination therapy was reported to be effective for vitiligo, a long-term evaluation is necessary to address the recurrence of vitiligo and the unexpected carcinogenic effects. The combination therapy is currently contraindicated in Japan.

Phototherapy with PUVA. Clinical question 4: Is PUVA therapy effective for vitiligo? Recommendation: PUVA therapy is effective for vitiligo. Grade of recommendation: B.

Psoralen plus UV-A therapy has been used to radiate vitiligo lesions for half a century. In 1996, the American Academy of Dermatology published the guideline of care for vitiligo.[33] PUVA has been applied more frequently after being recommended as the treatment for vitiligo,[33] although its efficacy and recurrence rates are somewhat controversial. In 2002, Kwok *et al.*[34] retrospectively evaluated the efficacy of PUVA therapy for vitiligo. They demonstrated that complete repigmentation was achieved in eight of 97 patients radiated by PUVA and that moderate repigmentation occurred in 59 of 97 patients.[34] They discussed the necessity of informed consent for recurrence, as they showed frequent re-depigmentation rates 1 year after PUVA therapy in 57 patients.[34] In Japan, PUVA therapy has been used for the treatment of vitiligo.

The grade of recommendation for the treatment of vitiligo with PUVA is B. Recent studies suggest that NB-UVB therapy is superior to PUVA therapy, with higher efficacy and lower recurrence of vitiligo and the occurrence of adverse reactions. NB-UVB therapy is more prevalent than PUVA therapy in Japan. Excess photo-radiation in PUVA therapy may induce phototoxic reactions and skin cancer. A subsequent guideline should include a consensus decision to limit the total sum and number of sessions of PUVA therapy.

Phototherapy with NB-UVB. Clinical question 5: Is NB-UVB therapy effective for vitiligo? Recommendation: NB-UVB therapy is effective for adult vitiligo and is the first-line phototherapy, as it is more effective than PUVA therapy. NB-UVB therapy is covered by Japanese public health insurance. Grade of recommendation: B.

Narrowband UV-B represents a symbol of a specific UVB wave, 311 ± 2 nm. NB-UVB therapy was initially used for the treatment of psoriasis in the 1980s, primarily in Europe. NB-UVB was subsequently applied for the treatment of vitiligo in the 1990s.[35–37] Four randomized, controlled trials using NB-UVB for vitiligo treatment have been reported.[25,35,38,39] Hamzavi *et al.*[25] performed a controlled study of 22 vitiligo patients that received NB-UVB therapy thrice weekly on one side and no treatment on the other side for 6 months, and demonstrated statistically significant repigmentation on the NB-UVB-radiated side ($P < 0.001$). However, the efficacy of repigmentation was diverse in the affected regions.[25] The affected lesions on the dorsa of hands and feet were less responsive to NB-UVB than the lesions on the trunk and extremities.[25] A placebo-controlled, double-blind study of 56 non-segmental vitiligo patients demonstrated that: (i) the color match of the repigmented skin was excellent in all patients in the NB-UVB group but in only 11 (44%) of those in the PUVA group ($P < 0.001$); (ii) that the improvement in the BSA affected by vitiligo was greater with NB-UVB therapy than with PUVA therapy in patients who completed 48 sessions ($P = 0.007$); and (iii) that the superiority of NB-UVB tended to be maintained 12 months after the cessation of therapy.[26] A study of 281 vitiligo patients reported that the treatment of vitiligo patients with UV-B radiation is as efficient as treatment with topical PUVA, and has fewer adverse reactions.[35]

The guideline for the diagnosis and management of vitiligo in the UK proposed that safety limits for NB-UVB for the treatment of vitiligo are more stringent than those applied to psoriasis, with an arbitrary limit of 200 treatments for skin types I–III.[39] This limit could be higher for skin types IV–VI at the discretion of the clinician and with the consent of the patient.[39]

Njoo *et al.*[36] studied NB-UVB therapy in 51 children with vitiligo that received twice weekly treatment for a maximum of 1 year, and concluded that NB-UVB therapy was effective and safe in childhood vitiligo and significantly improved the QOL. They recommended that NB-UVB therapy should be applied no longer than 12 months in children.[36] If no response is observed after 6 months, further therapy should be discouraged.[36] If, in responding cases, parents or patients insist on continuing treatment after 1 year, only limited areas should be exposed to NB-UVB radiation.[36] They advocated preventing unnecessary exposure to natural sunlight and using UV-blocking agents on sun-exposed areas.[36] In Japan, no evidence has been obtained regarding the efficacy and safety of NB-UVB therapy for childhood vitiligo. It is recommended that clinicians inform the parents and child patients of the probable effectiveness of NB-UVB therapy and the possible adverse reactions including carcinogenesis.

Currently, carcinogenetic adverse effects due to NB-UVB therapy have not well been elucidated in humans, as carcinogenesis occurs several decades after intense UV radiation. Experimental carcinogenesis has been examined in mice,[40] although the incidence of skin carcinomas varied with different NB-UVB radiation methods and strains of mice. Repeated radiation with the minimal erythema dose of NB-UVB induces more carcinogenesis than that of BB-UVB in mice.[40] NB-UVB therapy can induce repigmentation in vitiligo lesions with fewer radiation sessions than BB-UVB therapy.[41] Evidence is lacking to define the upper limit of radiation sessions for the treatment with NB-UVB for individuals with vitiligo, although the recommended limit of NB-UVB therapy is 12 months or 200 treatments.[36,39] UV exposure occurs during daily life. Therefore, history of sun exposure and sun-induced skin aging should be examined before starting phototherapy with NB-UVB. Dermatologists should decide on the therapeutic strategy of NB-UVB with consideration given to the likelihood of efficacy and adverse reactions. The current standard method for NB-UVB therapy is shown in Figure 5. A subsequent guideline should declare the limit of the total sum and number of sessions of NB-UVB treatment.

The grade of recommendation for the treatment of vitiligo with NB-UVB is B. Convincing results of NB-UVB treatment of vitiligo with evidence level III have been shown.

Phototherapy with 308-nm excimer laser/light. Clinical question 6: Is 308-nm excimer laser/light therapy effective for vitiligo? Recommendation: 308-nm excimer laser/light therapy can be applied to vitiligo lesions in which repigmentation are expected. The treatment features should fully be addressed. Grade of recommendation: C1.

To avoid radiation to the normal areas of skin, 308-nm excimer laser/light therapy can radiate 308-nm UV-B to targeted areas of vitiligo lesions. However, phototherapy requires a large amount of time to radiate huge vitiligo lesions. Therefore, 308-nm excimer laser/light therapy is useful for spotted and patched vitiligo lesions.

The efficacy of 308-nm excimer laser therapy in vitiligo is commonly reported as excellent (>75% repigmentation) in 15–50% of treated lesions.[42] A statistically significant improved response was observed in the UV-sensitive areas (face, neck, back, breast and arm) compared with UV-resistant areas (knees, elbows, wrists, hands, ankles and feet), when sessions were performed twice or thrice weekly for 4–36 weeks.[42] The ultimate rate of repigmentation appears to depend on the total number of sessions and not on their frequency.[43]

Adverse reactions to 308-nm excimer laser/light therapy include mild to severe erythema and occasional blisters. Long-

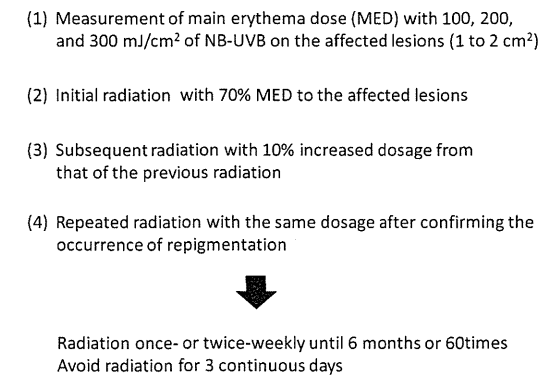

Figure 5. Example of narrowband ultraviolet B therapy.

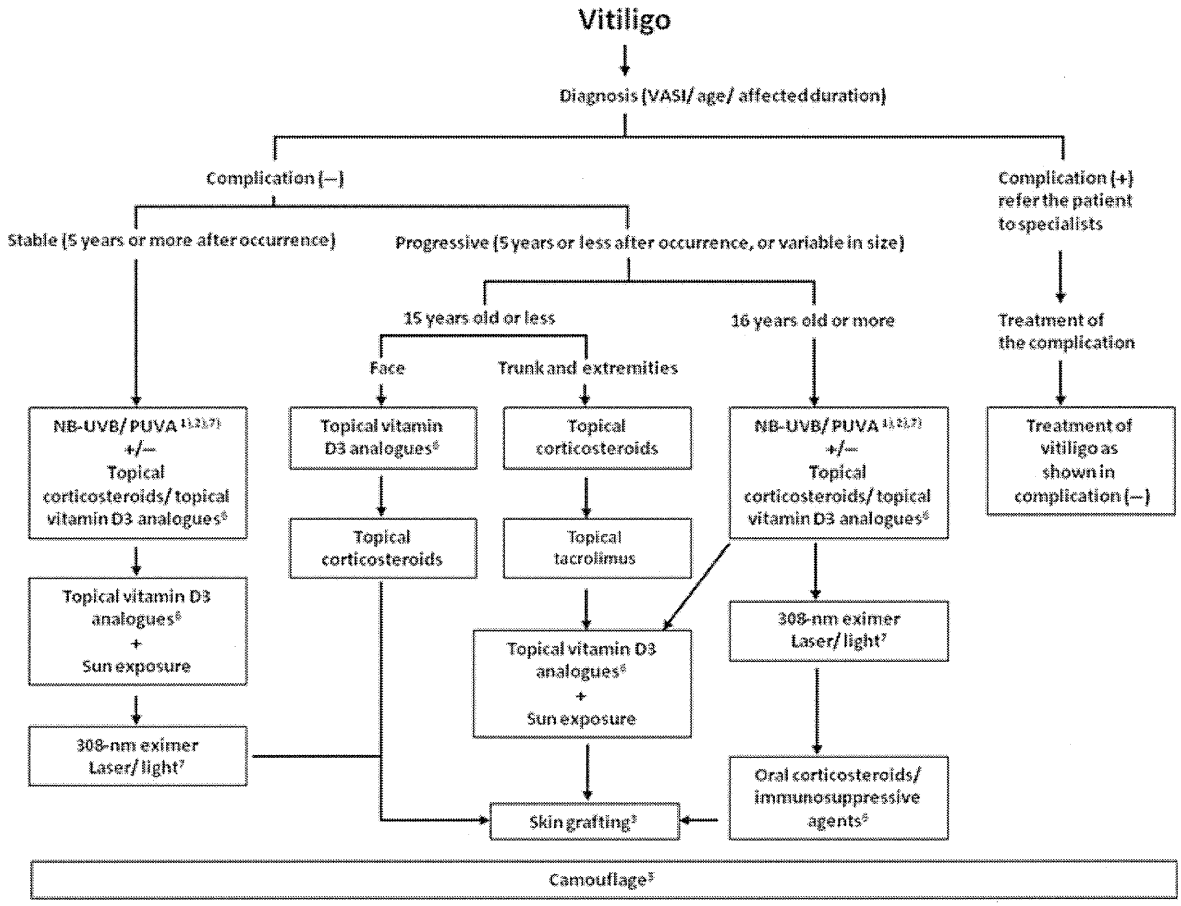

Figure 6. Proposed algorithm for the treatment of vitiligo in Japan. [1]Phototherapy depends on the equipment of each clinic or hospital. [2]Phototherapy should be initiated after considering the affected body surface area, the affected region and the required frequency of visit to each clinic or hospital. [3]Type of skin grafting could be chosen based on the opinion of affected patients after sufficient informed consent is obtained. [4]Combination of topical tacrolimus and phototherapy is currently forbidden in Japan. [5]Camouflage can be applied whenever affected patients wish to use the specific cosmetics. [6]Treatment is not covered by Japanese public health insurance. [7]Treatment should be used for patients aged 16 years or above. NB-UVB, narrowband ultraviolet B; PUVA, psoralen plus ultraviolet A therapy; VASI, Vitiligo Area Scoring Index. [Correction added on 28 March 2013, after first online publication: 'Topical corticosteroids', originally in the second box under 'Trunk and extremities', was changed to 'Topical tacrolimus'.]

standing adverse reactions are difficult to recognize. Long-term follow up of patients receiving 308-nm excimer laser/light therapy would be necessary to examine late-phase adverse reactions.

A randomized, investigator-blinded, half-side comparison study between 308-nm excimer light and NB-UVB phototherapy demonstrated an excellent response rate (>75% repigmentation) in 37.5% of vitiligo patients treated with 308-nm excimer light and in 6% of those treated with NB-UVB.[44]

It is difficult to integrate the findings from studies of 308-nm excimer laser/light therapy applied to vitiligo lesions because the protocols and instruments were different in each study. Furthermore, each study was not designed as a distinct randomized, controlled trial, and had less than 100 participants. In Japan, a controlled, prospective, randomized, double-blinded trial has not been conducted with a sufficient number of vitiligo patients. The efficacy and rate of adverse reactions remain uncertain for 308-nm excimer laser/light therapy in the Japanese population.

The grade of recommendation for the treatment of vitiligo with 308-nm excimer laser/light therapy is C1. This phototherapy can be applied for vitiligo lesions in which repigmentation are expected. Dermatologists using 308-nm excimer laser/light therapy should have enough knowledge of the treatment.

Oral corticosteroids. Clinical question 7: Are oral corticosteroids effective for vitiligo? Recommendation: Oral corticosteroids can be administrated for progressing vitiligo. Grade of recommendation: C1.

Corticosteroids may be administrated p.o. to patients with progressing vitiligo. Few reports with high levels of evidence have been shown. Kim *et al.*[45] studied the efficacy of low-dose oral corticosteroids for vitiligo with a protocol of p.o. prednisolone administration. The dose of oral prednisolone (0.3 mg/kg